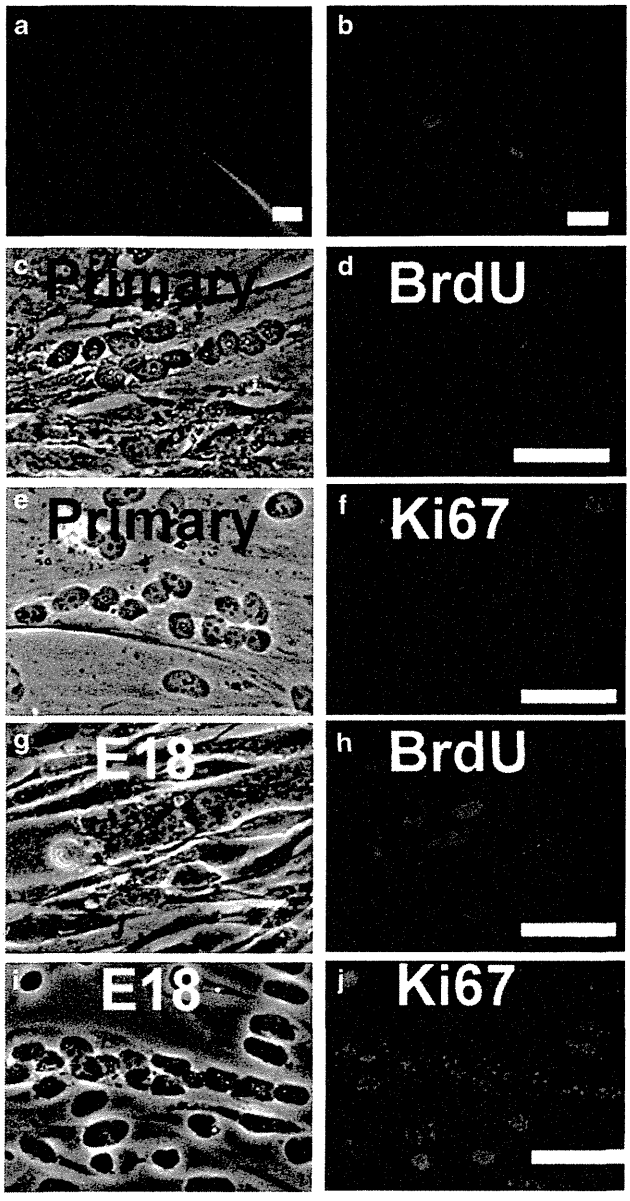

Figure 2 Nuclear progression in terminally differentiated immortalized human myogenic cells expressing telomerase and E7. (**a**, **b**) E18 cells were labeled with modified green fluorescent protein, and then 2.5×10^6 cells were transplanted into the TA muscles of NOD/Scid mice. (**a**) Whole TA muscles were recovered at 4 week after transplantation. Scale bar, 1 mm. (**b**) Pathological view of a TA muscle. Modified green fluorescent protein (green) was detected by immunofluorescence. Nuclei were stained with 2,4-diamidino-2-phenylindole dihydrochloride *n*-hydrate. Scale bar, 50 μm. (**c–j**) Primary cultured human myogenic cell Hu26 (**c–f**) and immortalized human myogenic cell clone E18 expressing telomerase and E7 (**g–j**) were cultured for up to 78 h in primary cultured myocyte differentiation medium. For the detection of DNA synthesis, cells were incubated with 10 μM 5-bromo-2′-deoxyuridine for the last 6 h of a 78-h differentiation culture (**c**, **d**, **g**, **h**). Phase contrast images (**c**, **e**, **g**, **i**) and immunofluorescence analysis with anti-5-bromo-2′-deoxyuridine antibody (red in **d**, **h**), or Ki67 (red in **f**, **j**) of the same fields are shown in each row. Nuclei were stained with 2,4-diamidino-2-phenylindole dihydrochloride *n*-hydrate (blue in **d**, **f**, **h**, **j**). Scale bars, 50 μm.

The single amino acid change in CDK4 prevented a cyclin-dependent kinase inhibitor, $p16^{INK4a}$, from inhibiting kinase activity of CDK4. Forced expression of CDK4R24C, cyclin D1 and hTERT efficiently expanded the lifespan of Hu5 cells and virtually immortalized Hu5 cells. Immortalized Hu5 derivatives expressing CDK4R24C and cyclin D1 under control of the human cytomegalovirus immediate early promoter were designated as Hu5/KD, whereas the cells expressing them under the control of the Tet-Off system were designated as Hu5/TKD. The pooled populations, Hu5/KD and Hu5/TKD, and their derivative clones, KD3 and TKD1, divided rapidly at a similar interval as primary myogenic cells did (Figures 3a–d). The expression of hTERT, CDK4R24C and cyclin D1 culminated in continuous cell proliferation for more than 200 population doublings (Figures 3e and f). In contrast to E7, the cell cycle drivers did not promote nuclear progression in terminally differentiated myotubes nor interfere with the cell cycle exit of myogenic progenitor cells under the differentiation-inducing condition (Figures 3g–k; Supplementary Figure 4). Hu5 derivatives transduced with recombinant lentiviruses encoding hTERT and CDK4R24C proliferated continuously but relatively slowly. Forced expression of hTERT and cyclin D1 did not immortalize Hu5 cells. We therefore concluded that the combined expression of the three genes immortalized human myogenic progenitor cells, resulting in restoration of their growth properties similar to that of primary cultured human myogenic cells.

Immortalized human myogenic cells preserve myogenic phenotype

To determine the karyotype of immortalized human myogenic cells at passages 18–30, about 22–32 metaphase spreads of each cell type were analyzed. The results show the cells maintained a normal 46XX diploid karyotype in both the immortalized populations and the immortalized clones (Figure 4).

High-level expression of CDK4 and cyclin D1 was observed in the immortalized cells (Figure 5a). pRb was highly phosphorylated under the growing condition. The cell cycle inhibitor $p16^{INK4a}$ remained at an extremely high level in the immortalized cells (Figure 5a). However, hypophosphorylated form of pRb was accumulated under the myogenic differentiation-inducing condition. Both the immortalized populations and the immortalized clones fused together and gave rise to myotubes. In addition, MyoD was highly expressed in the nuclei of myotubes (Figures 5b and c). The results here indicate that the immortalized clones KD3 and TKD1 preserved the myogenic phenotype represented by the previously immortalized Hu5 derivatives.[9]

Immortalized human myogenic cells retain differentiation potential both *in vivo* and *in vitro*

The cells immortalized by the forced expression of hTERT and E7 preserved the phenotypic characteristics of their parental Hu5 cells, including multipotentiality; one of the E7-expressing immortalized Hu5 cell clones, E18, retained the ability to undergo myogenic, osteogenic and adipogenic terminal differentiation.[7,9] The CDK4R24C and cyclin D1-expressing immortalized clones, KD3 and TKD1, also underwent myogenic, osteogenic and adipogenic terminal differentiation under the appropriate culture conditions (Figures 6a–c and f–h), although adipogenic differentiation was induced at relatively low efficiency.

To determine whether the immortalized human myogenic cells contributed to muscle regeneration *in vivo*, KD3 and TKD1 cells were transplanted into cardiotoxin-injected TA muscles of immunodeficient NOD/Scid mice. Before transplantation, KD3 and TKD1 cells were infected with a lentivirus vector encoding green fluorescent protein Venus. Transplanted cells were identified by the fluorescence of Venus and antibodies specific for green fluorescent protein. Transplanted KD3 and TKD1 cells (1×10^6 cells per TA) gave rise to many myofibers labeled with strong green fluorescence (8.6 ± 4.3 and

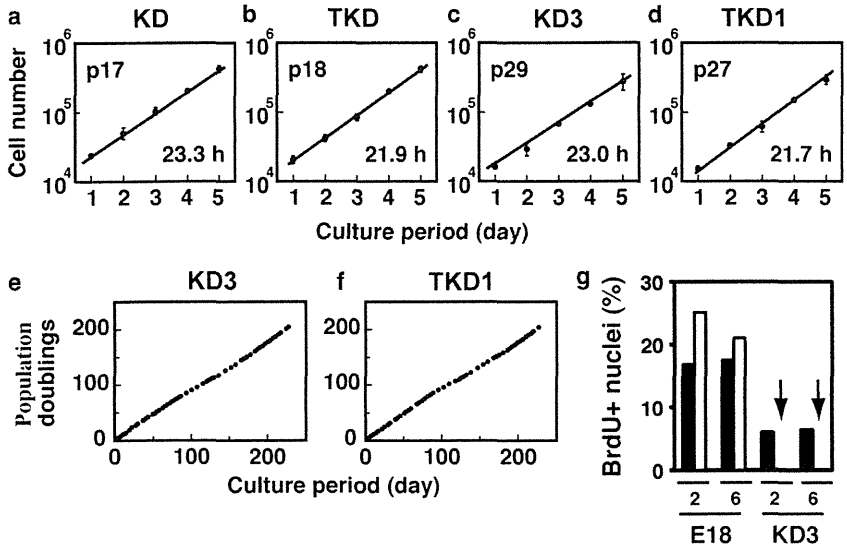

Figure 3 Proliferation of immortalized human myogenic cells. (**a–d**) Growth properties of a multiclonal population named KD, expressing hTERT, CDK4R24C and cyclin D1 under the control of a cytomegalovirus promoter (**a**), a multiclonal population named TKD, expressing hTERT, CDK4R24C and cyclin D1 under the control of a Tet-off system (**b**), a clone named KD3 isolated from KD (**c**) and a clone named TKD1 isolated from TKD (**d**). Passage numbers and doubling times are shown in the panels. (**e**, **f**) Life span plots of immortalized clones KD3 (**e**) and TKD1 (**f**). (**g**) E18 and KD3 cells were incubated with 10 μM 5-bromo-2′-deoxyuridine for the last 2 or 6 h of a 78-h culture in primary cultured myocyte differentiation medium. Ratios of 5-bromo-2′-deoxyuridine-positive nuclei in mononucleated progenitors (filled column) and myotubes (open column) were estimated from 1466–3196 nuclei of mononucleated progenitors and 404–1223 nuclei of myotubes, respectively. Numbers under the column represent the incubation time with 5-bromo-2′-deoxyuridine. Arrows represent the positions of open columns.

10.2 ± 9.1% of total TA myofibers, respectively) (Figures 6d and i). The relatively large s.d. in the present results was because of the low numbers of positive myofibers in the two specimens, probably due to leakage of the transferred cells to the injected TA muscle. Venus-positive myofibers were regenerated myofibers because they contained central nuclei (Figures 6e and j). No tumor was observed in the transplanted TA muscles. *In vitro* soft agar assay also showed that KD3 cells did not grow in an anchorage-independent way (Supplementary Figure 2). The results suggest that KD3 cells do not possess oncogenic potential. The ability of the immortalized human myogenic cells to regenerate muscle *in vivo* indicates that the immortalized cells established here represent a good model cell system for the fundamental and therapeutic study of human muscle development and disease.

Human myogenic cells recaptured proliferation capacity in cell-cycle driver-dependent manner

Both CDK4R24C and cyclin D1 were expressed under the control of the Tet-Off system in TKD1 cells. To determine the role of cell cycle drivers in the continuous proliferation of human myogenic cells, the expressions of CDK4R24C and cyclin D1 were suppressed by administration of doxycycline. Expression levels of CDK4 and cyclin D1 in TKD1 cells markedly declined during 5 days of incubation with doxcycline (Figure 7a). Doxcycline itself impaired neither the protein levels of either CDK4 or cyclin D1 in KD3 cells (Supplementary Figure 5) nor their DNA synthesis (Figures 7b–g). The number of proliferating TKD1 cells reduced following the decline in CDK4 and cyclin D1 proteins (Figures 7i, l). The morphology of doxycycline-treated TKD1 cells also became more flattened like senescent cells, and the nuclei looked thin during the cessation of proliferation (Figures 7h, j, k, m). In contrast, when doxycycline was removed from the culture, CDK4 and cyclin D1 were restored, and the proliferation capacity was completely recaptured by TKD1 cells (Figures 7a lane 4 and n–p). The results suggest that the proliferation capacity of human myogenic cells expressing hTERT is fully dependent on CDK4R24C and cyclin D1, and that before cellular senescence accompanied by telomeric attrition, human myogenic cells are capable of recapturing proliferation capacity.

Cryopreserved human myogenic cells derived from a disease muscle recapture proliferating activity by immortalization

Primary cultured human myogenic cells lose the ability to proliferate by degrees during culture *in vitro*. Cryopreserved primary cultured human myogenic cells obtained from Leigh disease muscle suffered from growth impairment accompanied by a prolonged cell cycle. One of the mortal cell clones from the primary cultured Leigh disease myogenic cells, HM2-5, which had a cell cycle of 73.5 h at passage 10 (Figure 8a), was infected with recombinant lentiviruses. Forced expression of hTERT, CDK4R24C and cyclin D1 had the cells dividing rapidly with a doubling time of 27.7 h (HM255, Figure 8b). A combination of hTERT and E7 also rescued the cells from growth impairment, but their doubling time (36.6 h) (HM253, Figure 8c) was longer than that of the clone immortalized by hTERT, CDK4R24C and cyclin D1. Both immortalized multiclonal populations HM253 and HM255 retained the ability to undergo terminal myogenic, osteogenic and adipogenic differentiation (Figures 8d–i). A cryopreserved mortal cell clone from muscle of another Leigh disease patient also recaptured its proliferation capacity and multipotentiality through immortalization by the combined expression of hTERT, CDK4R24C and cyclin D1 (Supplementary Figure 6). These results suggest that transduction of the three genes renders growth-impaired human myogenic cells proliferative and immortalized without loss of their differentiation potentialities.

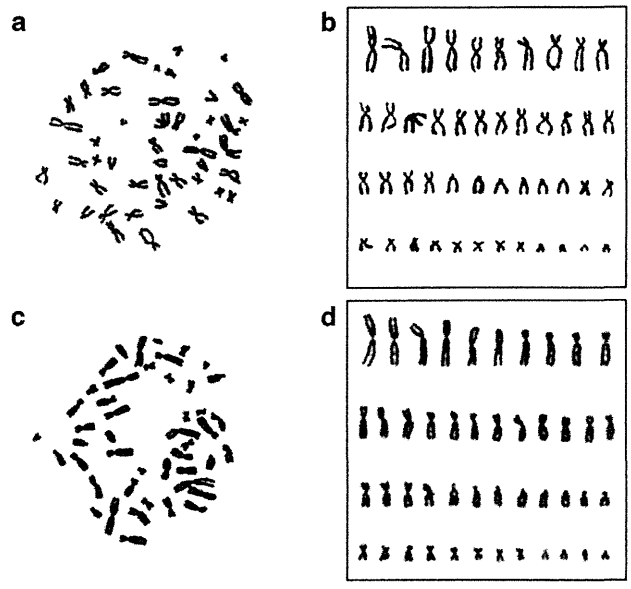

e	Diploid / Total	% Diploid
KD (p.18) (multiclonal)	30 / 32	93.8
KD3 (p.27) (monoclonal)	19 / 22	86.4
TKD (p.19) (multiclonal)	25 / 28	89.3
TKD1 (p.30) (monoclonal)	29 / 32	90.6

Figure 4 Karyotype analysis of immortalized human myogenic cells. Cells were treated with colcemid (2 μM) for 9 h. Metaphase chromosomes were visualized by Giemsa staining (**a**, **c**) and then aligned (**b**, **d**). Immortalized clones, KD3 (**a**, **b**) and TKD1 (**c**, **d**) and multiclones, KD and TKD (**e**), were analyzed.

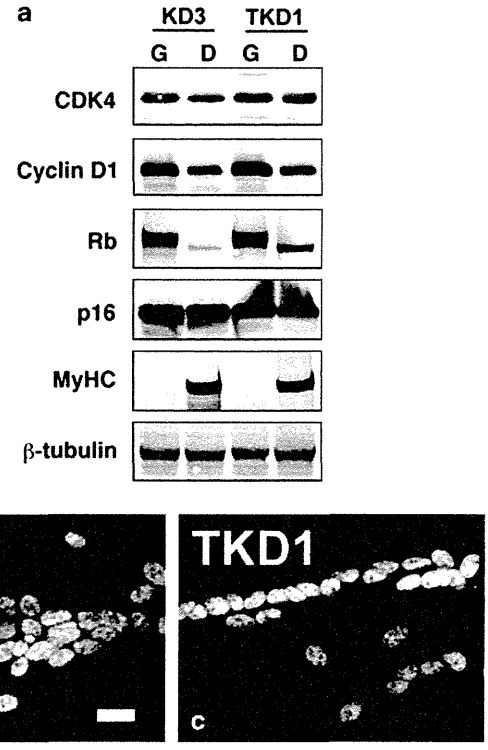

Figure 5 Expression patterns of growth- and differentiation-related proteins in immortalized human myogenic cells. (**a**) KD3 and TKD 1 cells were cultured in pmGM (g) or in primary cultured myocyte differentiation medium for 5 days (d). Fifteen micrograms of total proteins were subjected to immunobloting analysis with antibodies against CDK4, cyclin D1, Rb, $p16^{INK4a}$, myosin heavy chain and β-tubulin. (**b**, **c**) KD3 (**b**) and TKD1 (**c**) were cultured for 6 days in primary cultured myocyte differentiation medium and then subjected to immunofluorescence analysis with antibodies to MyoD. Scale bar, 20 μm.

DISCUSSION

Sarcopenia is an age-related loss of muscle mass leading to muscle weakness and atrophy. The slower regenerative capacity of aging muscle may be attributed to a decrease in the number and/or proliferation and differentiation capacities of muscle satellite cells. Actually, the number of satellite cells declines with age in humans.[16,17] In addition, the proliferation potential of human muscle satellite cells is limited by cellular senescence induced by progressive telomere shortening.[16,18] When the telomere length becomes less than about 5 kb, the Rb and p53 pathways are activated and culminate in irreversible growth arrest.[11,19,20] Cells also enter a state designated as stress or aberrant signal-induced senescence [18,20] (STASIS) or stress-induced premature senescence[21] (SIPS) that closely resembles replicative senescence when subjected to sub-lethal stress or oncogenic signals. The major characteristics of cells undergoing STASIS/SIPS are similar to those of replicatively senescent cells: the Rb and/or p53 pathways are activated and the cells stop proliferation. STASIS/SIPS can be induced in a telomere-independent way in human epithelial cells[11] and even in human fibroblasts,[12] although acceleration of telomere shortening is associated with STASIS/SIPS. Under conventional culture conditions, many types of human cells are likely to undergo precocious growth arrest before replicative senescence induced by telomere shortening,[22] though some types of human cells appear to be immortalized by the expression of hTERT alone without transformation of cell properties.[11,23,24] In fact, our previous and present studies strongly suggest that both inactivation of the Rb pathway and restoration of telomerase activity are required for efficient immortalization of human myogenic cells (Figure 9A). The growth arrest of primary cultured human myogenic cells may be attributable to an inadequate cellular context including culture conditions that stimulate the stress signaling pathway.[25]

Several previous studies emphasized that the age-related dysfunction of muscle is attributed to the age-related changes in environmental factors that attenuate the potential of muscle satellite cells. Transplantation of whole muscles between old and young rats shows that the regenerative capacity of aged muscle is enhanced when grafted into young muscle.[26] The decrease of circulating growth factors[27] and the number of motor units[28] are candidates for the responsible environmental factors or age-related changes in skeletal muscle. In addition, primary cultured human myogenic cells derived from skeletal muscles of aged persons (>75 years old) show growth properties similar to those of the myogenic cells obtained from younger persons under the appropriate culture conditions (Supplementary Figure 3A) (Hashimoto and Okamura, unpublished data). On the other hand, a previous study showed that myogenic cells from

aged muscle demonstrated less ability to proliferate in primary cultures.[6] Given that myogenic cells derived from an aged human are fragile and likely to lose proliferation potential under inappropriate culture conditions, these different results under different culture conditions are plausible. Actually, we have found that the proliferation capacity of human and mouse primary myogenic cells maintained in a medium containing DMEM is higher than that of the cells maintained in a medium containing Ham's F10, even though an F10-based medium was used to isolate and culture primary myogenic cells in many studies.[6,29]

Muscle-degenerative diseases such as muscular dystrophies provoke extensive replication of human muscle satellite cells.[30] Satellite cells in regenerating muscles also suffer from cellular stresses including those induced by inflammatory cytokines. Therefore, precocious growth arrest, as well as the replicative senescence of satellite cells, is likely to cause the loss of muscle-regenerative capacity in muscle-degenerative diseases. Results obtained by previous and present studies indicate a possibility of a new therapeutic strategy for sarcopenia and muscular dystrophy that overcomes the precocious growth arrest triggered by the Rb pathway. Human myogenic cells are vulnerable to cellular stresses and more likely to undergo premature growth arrest than human foreskin fibroblasts because primary cultured human fibroblasts undergo precocious growth arrest/STASIS/SIPS exclusively when exposed to stress inducers such as H_2O_2 and ultraviolet light.[21] From this point of view, the Rb pathway in human myogenic cells will be an attractive target of therapeutic intervention in muscle-degenerative diseases. The present study also shows that the total amount of pRb declined during growth arrest in primary human myogenic cells at later passages, immortalized human myogenic cells undergoing myogenesis and TKD1 cells stimulated with doxycycline. Therefore, we should consider both quantitative and qualitative control of pRb during precocious growth arrest.

The present results suggest that suppression of the Rb signaling pathway is required for immortalization of human myogenic cells in addition to telomere restoration (Figures 9Ba–f). Either Bmi-1 (ref. 9) or wild-type CDK4 (ref. 13) was coexpressed with hTERT in primary cultured human myogenic cells to block the $p16^{INK4a}$ signaling pathway, but the cells did not undergo immortalization. The results indicate that neither Bmi-1 nor the wild-type CDK4 alone allows hTERT to immortalize human myogenic cells, and that immortalization of human myogenic cells still requires secondary changes under these conditions. In fact, the combined expression of wild-type CDK4 and hTERT or Bmi-1 and hTERT results in immortalization of human myogenic cells exclusively under the optimized culture conditions supplemented with dexamethasone and growth factors,[13,14] although the role of those supplements has been unknown. It is conceivable that CDK4 kinase activity released from the inhibition by $p16^{INK4a}$ is not high enough to hyperphosphorylate Rb (Figures 9Bc and d). In contrast, CDK4R24C allows hTERT to promote slow, but continuous, proliferation in primary cultured human myogenic cells (Figure 9Be). CDK4R24C contributes to hyperphosphorylation of Rb, whereas the contribution of forced expression of wild-type CDK4 is quite limited because $p16^{INK4a}$ inhibits the kinase activity of wild-type CDK4. Our previous study indicated that E7 prevents Rb independently of $p16^{INK4a}$ and leads to immortalization of hTERT-expressing human myogenic cells[9] (Figure 9Bb). Given that the suppression of Rb, but not $p16^{INK4a}$, is quite effective in immortalization of human myogenic cells, we concluded that complete inhibition of both Rb activation and telomere shortening is necessary and sufficient for immortalization of human myogenic cells.

Combined expression of CDK4R24C, cyclin D1 and hTERT successfully and reproducibly immortalized human myogenic cells derived from normal and disease muscles, resulting in rapid proliferation without compromising differentiation potential. Cyclin D1 has a crucial role as a limiting factor of CDK4 kinase activity. Forced expression of cyclin D1 increases CDK4R24C kinase activity to an extent that is relevant for hyperphosphorylation of Rb, which then results in rapid proliferation, possibly due to the potent inhibition of Rb function (Figure 9Bf). The slower cycling of human myogenic cells immortalized by either E7 or CDK4R24C and hTERT also implies that higher CDK4 activity is required for rapid proliferation (Figures 9Bb and e). However, we cannot exclude a possibility that extraordinarily high activity of the CDK4R24C/cyclin D1 complex results in the phosphorylation of putative off-target substrates that have an essential role in the cell cycle progression and are usually phosphorylated by another member of the CDK family (Figure 9Bf).

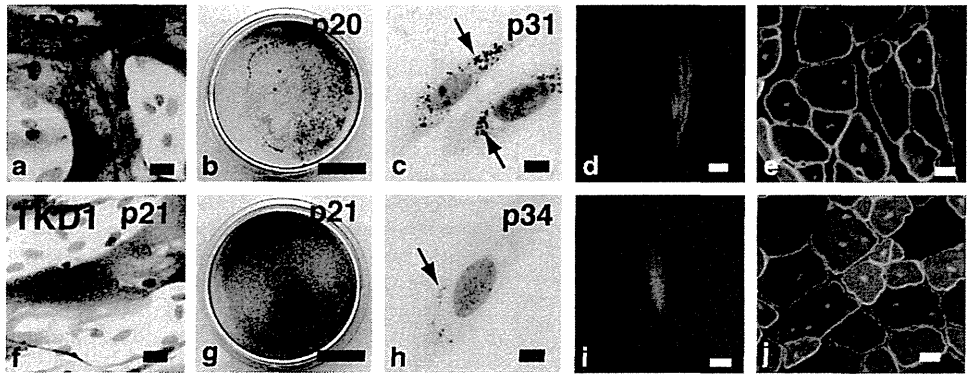

Figure 6 Multipotentiality of immortalized human myogenic cell clones KD3 and TKD1. KD3 (**a–e**) and TKD1 (**f–j**) were induced to undergo myogenic, osteogenic and adipogenic differentiation. (**a, f**) Cells were cultured for 5 days in primary cultured myocyte differentiation medium. Myosin heavy chain was detected by immunostaining with a horseradish peroxidase reaction. Nuclei were detected with staining with hematoxylin (blue). Scale bar, 50 μm. (**b, g**) The cells were cultured for 9 days in serum-containing medium supplemented with β-GP (10 mM). The cells were then stained with Alizarin Red S. Whole 35-mm dishes are shown. Scale bar, 10 mm. (**c, h**) The cells were cultured for 5 days in serum-containing medium supplemented with γ-linolenic acid (100 μM). Numerous lipid droplets (arrows) were stained with Oil Red O. Nuclei were detected by staining with hematoxylin (blue). Scale bar, 10 μm. (**d, e, i, j**) KD3 (**d, e**) and TKD1 (**i, j**) cells were labeled with modified green fluorescent protein and then 1×10^6 cells were transplanted into the TA muscle of NOD/Scid mice. (**d, i**) Whole TA muscles were recovered at 4 weeks after transplantation. Scale bars, 1 mm. (**e, j**) Pathological views (**d, i**). Modified green fluorescent protein (green) and laminin α2 (red) were detected by immunofluorescence. Nuclei were stained with 2,4-diamidino-2-phenylindole dihydrochloride *n*-hydrate. Passage numbers of cells are shown in (**a–c** and **f–h**). Scale bar, 20 μm.

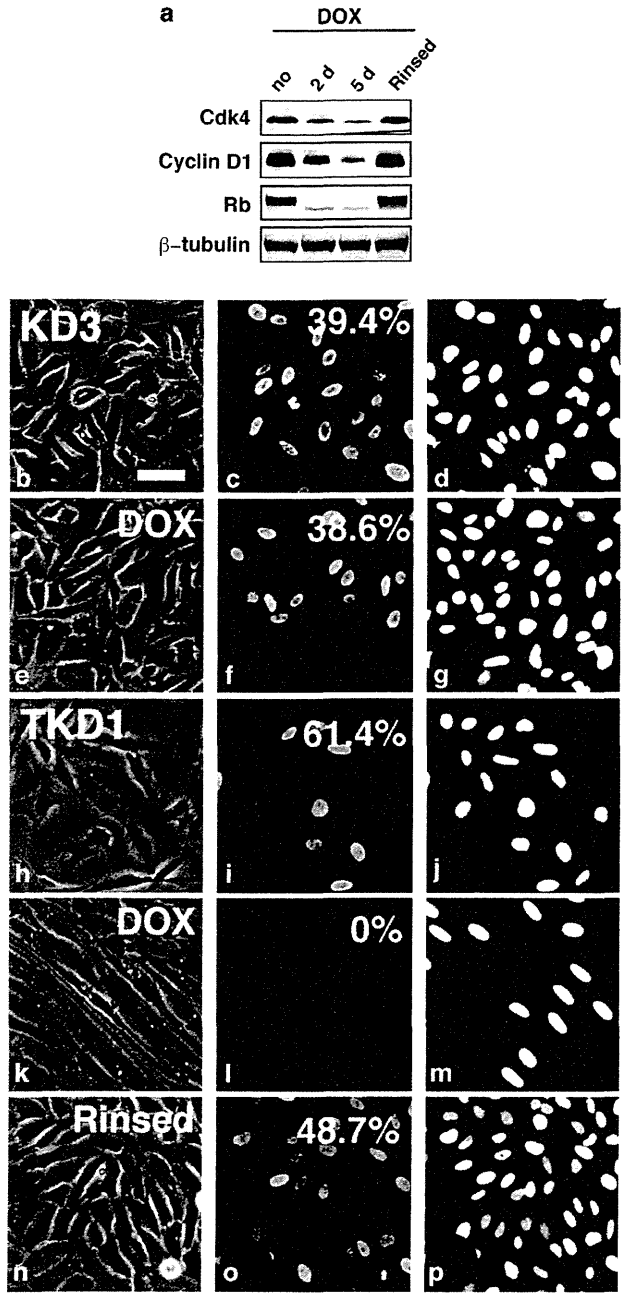

Figure 7 Reversible and precocious growth arrest induced by doxycycline in TKD1. (**a**) Fifteen micrograms of total proteins were subjected to immunobloting analysis with antibodies against CDK4, cyclin D1, Rb and β-tubulin. TKD1 cells were cultured for 2 days in medium containing 0.1% ethanol (vehicle) (lane 1), and for 2 days (lane 2) or 5 days (lane 3) in pmGM containing 250 nM doxycycline. For the recovery of CDK4 and cyclin D1, doxycycline was removed from the TKD1 culture after 5 days doxycyline treatment (lane 4). (**b–g**) KD3 cells were cultured for 2 days in medium containing 0.1% ethanol (vehicle) (**b–d**) or for 2 days in medium containing 250 nM doxycycline (**e–g**). TKD1 cells were cultured for 2 days in medium containing 0.1% ethanol (**h–j**), for 5 days in medium containing 250 nM doxycycline (**k–m**) or for 4 days in doxycycline-free medium following 5 days of culture in medium containing doxycycline (**n–p**). The cells were incubated for the last 6 h of culture in medium containing 10 nM 5-bromo-2′-deoxyuridine. The percentage of 5-bromo-2′-deoxyuridine-positive nuclei/total nuclei is shown in the panels (**c, f, i, l, o**). Phase contrast images (**b, e, h, k, n**), immunofluorescence analysis with anti-5-bromo-2′-deoxyuridine antibody (**c, f, i, l, o**), and nuclear staining with 2,4-diamidino-2-phenylindole dihydrochloride *n*-hydrate (**d, g, j, m, p**) of the same fields are shown in each row. Scale bar, 50 μm.

Forced expression of CDK4R24C and cyclin D1 did not affect the differentiation potential of human myogenic cells, although forced expression of cyclin D1 alone inhibits myogenesis of the mouse myoblastic cell line C2C12.[31,32] Rb was completely dephosphorylated during the differentiation culture, even though CDK4R24C and cyclin D1 still remained at high levels in the immortalized human myogenic cells. CDK inhibitors $p21^{cip1}$ and $p27^{kip1}$ are unlikely to be involved in the suppression of CDK4R24C activity during terminal muscle differentiation because the amount of the inhibitors does not increase in human myogenic cells (Shiomi and Hashimoto, unpublished data). Therefore, the present results imply another novel pathway leading to the suppression of CDK4/cyclin D1 activity at the post-translational level in human myogenic cells.

Immortalized human myogenic cells that preserve normal differentiation potential have been reported in two previous studies.[9,13] However, the previously established human myogenic cell clones require 36–48 h for doubling, whereas primary cultured human myogenic cells divide every 20–30 h. In addition, one of them also required additional supplementation of the multifunctional steroid dexamethasone and hepatocyte growth factor, whose roles in immortalization process are unknown.[13] The other was established in our previous study with the use of oncogene product E7 for immortalization.[9] In contrast to previous ones, the present human myogenic cell clones retain a growth property similar to that of primary cultured human myogenic cells in the early passages, multipotentiality and normal diploid chromosomes. Therefore, the immortalized normal myogenic cells established in the present study are the human equivalent to mouse myogenic cell lines, and will contribute to fundamental and therapeutic studies.

The novel immortalization method established in the present study is more reliable and reproducible than the previously reported methods. We have succeeded in immortalization of several primary cultured human myogenic cells independently obtained from normal and diseased muscles including Duchenne muscular dystrophy and Fukuyama congenital muscular dystrophy (Hashimoto, unpublished data). Immortalized human myogenic cells from different neuromuscular diseases are currently being established in our laboratories and those of our collaborators. Human cell models of various neuromuscular diseases will contribute to causal analysis of symptoms and therapeutic approaches of rare diseases.

MATERIALS AND METHODS

Isolation and culture of human myogenic cells

The human myogenic cell clone Hu5 was isolated from normal subcutaneous muscle tissue of a 42-year-old woman,[4] and other human myogenic cells were obtained from normal abdominal muscle tissues of a 75-year-old man (Hu20, passage 2; A), a 50-year-old man (Hu21), a 69-year-old man (Hu23) and a 65-year-old man (Hu26). To prepare primary cultured human myogenic cells, muscle fragments were minced, digested with TrypLE Express (Invitrogen, Carlsbad, CA, USA) and then a small amount of cells obtained from 20–40 mg muscle were plated on a 90-mm dish coated with type I collagen (Sumilon, Tokyo, Japan). The cells were maintained at 37°C under 10% CO_2 in dishes coated with type I collagen and containing primary cultured myocyte growth medium (pmGM) consisting of Dulbecco's modified Eagle's medium (DMEM) supplemented with 20% fetal bovine serum (FBS), 2% Ultroser G (Biosepra, Cedex-Saint-Christophe, France) and glucose (4.5 mg ml^{-1}). Cells were plated at 2×10^5 per 90-mm dish and cultured in pmGM. For induction of myogenic differentiation, the medium was changed to primary cultured myocyte differentiation medium after 48 h of culture; it consists of the chemically defined medium TIS[33,34] supplemented with 2% FBS.

For induction of terminal osteogenic differentiation, cells were cultured in DMEM supplemented with 10% FBS, glucose (4.5 mg ml^{-1}) and 10 mM β-glycerophosphate (β-GP) (Sigma, St Louis, MO, USA) alone. The cells were

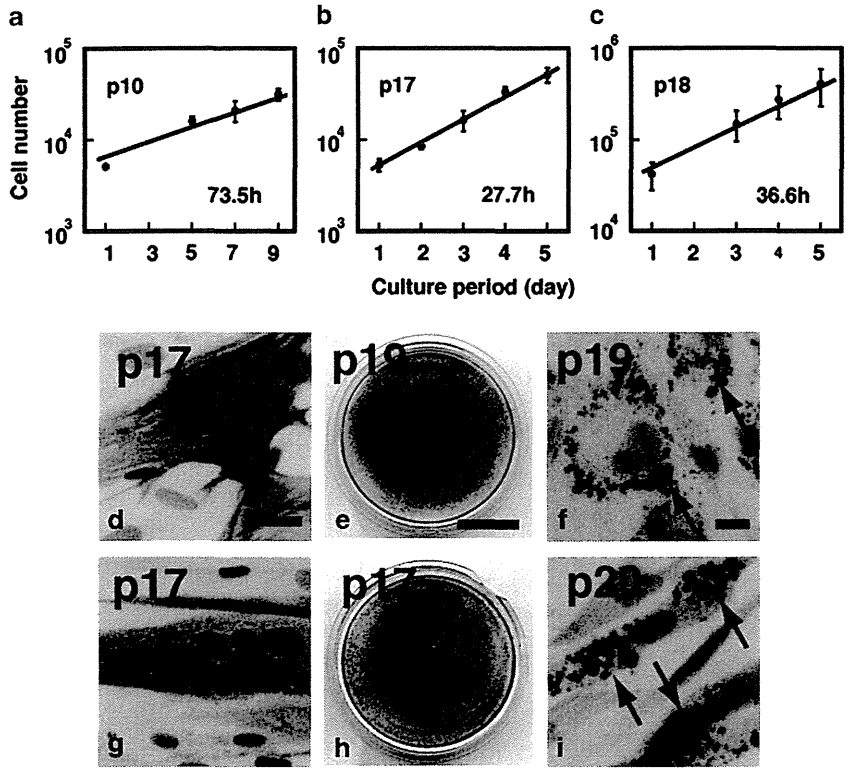

Figure 8 Recapture of proliferation capacity by myogenic cells derived from human muscle diseases. (**a–c**) Growth properties of primary cultured human myogenic cell clone HM2-5 obtained from muscle of a Leigh disease patient (**a**), immortalized clone HM255 derived from HM2-5 established by transduction with hTERT, CDK4R24C and Cyclin D1 (**b**), and immortalized clone HM253 derived from HM2-5 established by transduction with hTERT and E7 (**c**). Passage numbers and the doubling time were shown in the panels. (**d–i**) Multipotentiality of immortalized human myogenic cell clones derived from Leigh disease patients. HM255 (**d–f**) and HM253 (**g–i**) were induced to undergo myogenic, osteogenic and adipogenic differentiation. (**d, g**) Cells were cultured for 5 days in primary cultured myocyte differentiation medium. Myosin heavy chain was detected by immunostaining with a horseradish peroxidase reaction product. Nuclei were detected with staining with hematoxylin. Scale bar, 50 μm. (**e, h**) Cells were cultured for 9 days in serum-containing medium supplemented with β-GP (10 mM). Cells were then stained with Alizarin Red S. Whole 35-mm dishes are shown. Scale bar, 10 mm. (**f, i**) The cells were cultured for 5 days in serum-containing medium supplemented with γ-linolenic acid (100 μM). Numerous lipid droplets (arrows) were stained with Oil Red O. Nuclei were detected with staining with hematoxylin. Passage numbers of cells were shown in (**d–i**). Scale bar, 10 μm.

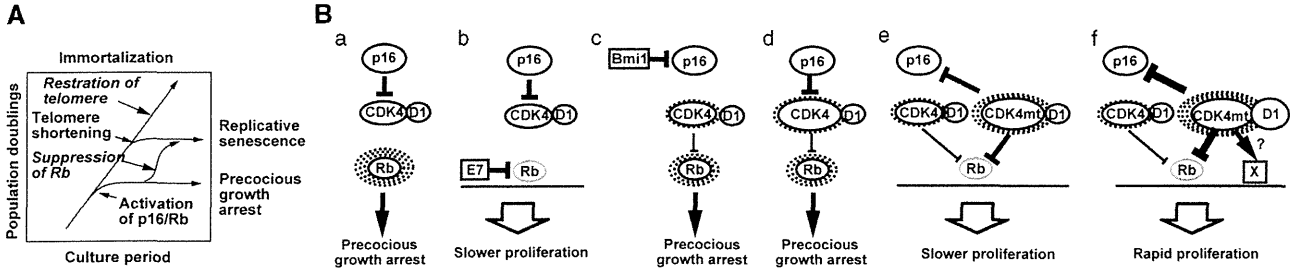

Figure 9 Premature growth arrest and replicative senescence of human myogenic cells. (**A**) Putative stress-induced activation of the $p16^{INK4a}$–Rb pathway triggers precocious growth arrest, independent of telomere shortening. Human myogenic cells under this state are able to recapture proliferation capacity by suppression of the Rb pathway. Telomere shortening also triggers activation of the Rb pathway and leads the cells to enter the irreversible growth arrest called replicative senescence. (**B**) Mechanistic scheme of suppression of precocious growth arrest by mutant CDK4 (CDK4R24C) and cyclin D1. (a) Putative stress-induced activation of $p16^{INK4a}$ inhibits endogenous CDK4, resulting in precocious growth arrest. (b) Papillomavirus type 16 gene *E7* suppresses Rb independently of p16. (c) Bmi-1 inhibits p16 expression. Endogenous CDK4 does not completely suppress Rb. (d) Forced expression of wild-type CDK4 sequesters p16, but does not completely suppress Rb because its kinase activity is inhibited by p16. (e) Forced expression of CDK4R24C sequesters p16, severely suppresses Rb, and allows human myogenic cells to proliferate slowly because CDK4R24C is not inhibited by p16. (f) Combined expression of CDK4R24C and cyclinD1 sequesters p16, induces hyperphosphorylation of Rb and allow human myogenic cells to proliferate rapidly, because the amount of cyclin D1 limits CDK4 kinase activity. A possibility that extraordinarily high activity of the CDK4R24C/cyclin D1 complex results in the phosphorylation of putative off-target substrates (represented as 'X') cannot be excluded. A putative action of the CDK4R24C/Cyclin D1 is represented as '?'. Dotted circles represent functional activity of Rb and CDK4.

stained with the calcium dye Alizarin Red S (2%, Sigma).[4] Images of stained dishes were obtained with a digital scanner (GT-9700F; Epson, Osaka, Japan) and then post-processed using Adobe Photoshop (Adobe Systems, San Jose, CA, USA). To induce adipogenic differentiation, we cultured myogenic cells in DMEM supplemented with 10% FBS, glucose (4.5 mg ml^{-1}) and 100 μM γ-linolenic acid (Sigma) for up to 5 days. The cells were stained with 0.3% Oil Red O (Sigma).[4]

Multiclonal populations of primary cultured myogenic cells HM1 and HM2, which were originally registered as M06-736 and M07-635, were obtained from biceps brachii muscles of Leigh disease patients, who were 3-month- and 5-year-old males, at the National Center of Neurology and Psychiatry (Kodaira, Japan). The mortal clones HM1-8 and HM2-5 were isolated from HM1 and HM2, respectively, at the National Center for Geriatrics and Gerontology. HM1 and HM2 had been cultured at 37°C under 5% CO_2 in non-coated standard tissue culture dishes containing DMEM/Ham's F12=1:1 supplemented with 20% FBS and glucose (4.5 mg ml^{-1}) alone, and cryopreserved at the National Center of Neurology and Psychiatry. The cells were cultured under the same conditions as Hu5 in the present study.

Viral vector construction and viral transduction

Lentiviral vector plasmids were constructed by recombination using the Gateway system (Invitrogen). Briefly, the EF1a promoter in CSII-EF-RfA (a gift from Dr H Miyoshi, RIKEN) was replaced with a tetracyclin-inducible promoter, TRE-Tight, from pTRE-Tight (Clontech, Mountain View, CA, USA) to generate CSII-TRE-Tight-RfA. Human cyclin D1 and human mutant CDK4 (CDK4R24C: an INK4a resistant form of CDK4, generously provided by Dr E Hara) were first recombined into entry vectors by a BP reaction (Invitrogen). Then these segments were recombined with CSII-TRE-Tight-RfA by an LR reaction (Invitrogen) to generate CSII-TRE-Tight-cyclin D1 and -CDK4R24C. The rtTA segment from pTet-Off Advanced (Clontech) was amplified by PCR and first recombined with the donor vector pDONR221 by BP reaction (Invitrogen) to generate pENTR221-TetOff, and then recombined with a lentiviral vector, CSII-CMV-RfA, by LR reaction (Invitrogen) to generate CSII-CMV-TetOff. Construction of CSII-CMV-cyclin D1, -CDK4R24C and -hTERT was described previously.[35] The recombinant lentiviruses with the vesicular stomatitis virus G glycoprotein were produced as described previously.[36] The recombinant retroviruses encoding hTERT and E7 were produced as described previously.[9,37]

Hu5, HM1-8 and HM2-5 cells were transduced with recombinant lentiviruses and retroviruses as described.[9,11,35] Following inoculation with viruses, the continuously proliferating cells were selected without drug treatment.

For single-cell cloning, transfected Hu5 cells were suspended at 5 cells per ml, and then 100 µl of the cell suspension was dispensed to each well of a 96-well plate coated with collagen, so that each well contained zero or one cell. Single-cell-derived clones were isolated and expanded for experimentation. The immortalized human myogenic cell clone KD3 will be available from RIKEN BioResorce Center (http://www.brc.riken.go.jp).

Analysis on growth properties

In total, 2000 cells were plated per well of a 12-well plate coated with type I collagen. Cells were collected and cell numbers were counted every 24 h between days 3 and 8 of culture in pmGM. Averages and s.d.'s of cell numbers per well from three independent wells were estimated.

To detect synthesizing DNA, cells were incubated with 10 µM 5-bromo-2′-deoxyuridine (Sigma) for the last 6 h of each culture, fixed in paraformaldehyde for 10 min and then subjected to immunofluorescence analysis after denaturation of DNA with 2 M HCl and neutralization with 0.1 M $Na_2B_4O_7$ according to the manufacturer's instructions (Roche Diagnostics, Indianapolis, IN, USA).

Karyotyping

After incubation in pmGM supplemented with 2 µM colcemid at 37°C for 6 h, cells were trypsinized and incubated in 0.5 ml of 1% sodium citrate for 15 min. This was followed by addition of 0.5 ml of Carnoy's fixative (methanol/acetic acid, 3:1 by volume). The fixed cells were then spun down and resuspended in 0.5 ml of Carnoy's fixative. Metaphase chromosomes were stained with 10% Giemsa solution (Wako Pure Chem., Osaka, Japan) for 10 min.

Immunobloting analysis

Sample preparation and immunoblot analysis were performed as previously described.[33,34,38] Immune complexes were detected by colorimetry with a BCIP/NBT detection kit (Nacalai, Kyoto, Japan) or an ECL kit (GE Healthcare, Piscataway, NJ, USA). Primary antibodies included mouse monoclonal antibodies to chicken sarcomeric myosin heavy chain (MF20, undiluted culture supernatant),[39] p16^{INK4a} (BD Bioscience, Franklin Lakes, NJ, USA), p21^{cip1} (Merk KGaA, Darmstadt, Germany), p53 (Merk), Rb (BD Bioscience), CDK2 (8A12, Medical Biological Laboratory, Nagoya, Japan), cyclin D1 (BD Bioscience) and β-tubulin (GE Healthcare), and a rabbit polyclonal antibody to CDK4 (Hashimoto, unpublished). Secondary antibodies included alkaline phosphatase (DAKO, Carpinteria, CA, USA)—or horseradish peroxidase (GE Healthcare)—labeled antibodies to mouse or rabbit immunoglobulin G. Immune complexes on the PVDF membranes (Fluoro Trans W; Pall, Port Washington, NY, USA) were scanned with a digital scanner (GT-9700F; Epson) or LAS-4000 IR multicolor (Fujifilm, Tokyo, Japan) and then post-processed using Adobe Photoshop (Adobe Systems).

Transplantation of human myogenic cells

Immortalized human myogenic cells were labeled with modified Venus green fluorescent protein by transduction with a lentivirus vector, CSII-CMV-MCS-IRES2-Venus (kindly provided by Dr Miyoshi). Tibialis anterior (TA) muscles of 10-week-old female NOD/Scid mice were injected with 20 µl of 10 µM cardiotoxin (Wako Pure Chem.).[40] On the next day, 1×10^6 of the Venus-labeled cells suspended in 30 µl of L-15 (Sigma) were transplanted into the regenerating TA muscle. At 4 weeks after transplantation, the TA muscles were removed and quickly frozen in isopentane cooled with liquid nitrogen and processed for preparation of cryosections as described.[41] Muscle specimens were sectioned at a thickness of 7 µm with a cryostat.

Immunofluorescence analysis

The frozen sections and cultured cells were fixed with 4% paraformaldehyde at 4°C for 30 or 10 min, respectively, and then incubated with primary antibodies. Primary antibodies included those to mouse monoclonal antibodies to mouse MyoD (5.8A, 1:10 dilution, Novocastra, Newcastle, UK), myosin heavy chain (undiluted supernatant), laminin α2 (1:100 dilution, Enzo Life Science, Farmingdale, NY, USA), 5-bromo-2′-deoxyuridine (1:50 dilution, Roche Diagnostics) and rabbit polyclonal antibodies to green fluorescent protein (1:500 dilution, Medical Biological Laboratory) and Ki-67 (1:2 dilution, YLEM, Rome, Italy). Secondary antibodies were biotinylated Alexa 488 or Cy3-labeled antibodies to mouse, rat (Jackson ImmunoResearch Laboratory, Bar Harbor, ME, USA) or rabbit (Molecular Probes, Eugene, OR, USA). The biotinylated antibodies were detected with streptavidin-conjugated horseradish peroxidase. The peroxidase reaction was performed with 3,3-diaminobenzidine (Sigma). Cell nuclei were stained with 2,4-diamidino-2-phenylindole dihydrochloride *n*-hydrate (1.0 µg ml^{-1}, Sigma) or hematoxylin (Wako). Samples were visualized using an upright microscope (model BX50; Olympus, Tokyo, Japan) and a CCD camera (DP70; Olympus), or an inverted microscope (model IX71; Olympus) and a CCD camera (DP70; Olympus). Images were post-processed using Adobe Photoshop (Adobe Systems).

Suppression and induction of gene expression using Tet-Off system

TKD1 cells (5×10^4 cells per 35-mm dish) were cultured for 2 days in pmGM and then the medium was changed to pmGM supplemented with 250 nM doxycycline (Sigma). To remove doxycyline from the culture, the cells were replated twice and cultured in pmGM (Roche Diagnostics) according to the manufacturer's instructions.

CONFLICT OF INTEREST

The authors declare no conflict of interest.

ACKNOWLEDGEMENTS

We thank H Miyoshi for providing lentivirus vectors. This study was supported by grants to NH and TK from the Ministry of Health, Labor and Welfare of Japan.

1 Kuang S, Charge SB, Seale P, Huh M, Rudnicki MA. Distinct roles for Pax7 and Pax3 in adult regenerative myogenesis. *J Cell Biol* 2006; **172**: 103–113.
2 Oustanina S, Hause G, Braun T. Pax7 directs postnatal renewal and propagation of myogenic satellite cells but not their specification. *EMBO J* 2004; **23**: 3430–3439.

3 Yaffe D, Saxel O. Serial passaging and differentiation of myogenic cells isolated from dystrophic mouse muscle. *Nature* 1977; **270**: 725–727.
4 Wada MR, Inagawa-Ogashiwa M, Shimizu S, Yasumoto S, Hashimoto N. Generation of different fates from multipotent muscle stem cells. *Development* 2002; **129**: 2987–2995.
5 Mukai A, Hashimoto N. Localized cyclic AMP-dependent protein kinase activity is required for myogenic cell fusion. *Exp Cell Res* 2008; **314**: 387–397.
6 Decary S, Mouly V, Hamida CB, Sautet A, Barbet JP, Butler-Browne GS. Replicative potential and telomere length in human skeletal muscle: implications for satellite cell-mediated gene therapy. *Hum Gene Ther* 1997; **8**: 1429–1438.
7 Hashimoto N, Kiyono T, Wada MR, Umeda R, Goto Y, Nonaka I *et al.* Osteogenic properties of human myogenic progenitor cells. *Mech Dev* 2008; **125**: 257–269.
8 Bigot A, Jacquemin V, Debacq-Chainiaux F, Butler-Browne GS, Toussaint O, Furling D *et al.* Replicative aging down-regulates the myogenic regulatory factors in human myoblasts. *Biol Cell* 2008; **100**: 189–199.
9 Hashimoto N, Kiyono T, Wada MR, Shimizu S, Yasumoto S, Inagawa M. Immortalization of human myogenic progenitor cell clone retaining multipotentiality. *Biochem Biophys Res Commun* 2006; **348**: 1383–1388.
10 Seigneurin-Venin S, Bernard V, Tremblay JP. Telomerase allows the immortalization of T antigen-positive DMD myoblasts: a new source of cells for gene transfer application. *Gene Therapy* 2000; **7**: 619–623.
11 Kiyono T, Foster SA, Koop JI, McDougall JK, Galloway DA, Klingelhutz AJ. Both Rb/p16INK4a inactivation and telomerase activity are required to immortalize human epithelial cells. *Nature* 1998; **396**: 84–88.
12 Gorbunova V, Seluanov A, Pereira-Smith OM. Expression of human telomerase (hTERT) does not prevent stress-induced senescence in normal human fibroblasts but protects the cells from stress-induced apoptosis and necrosis. *J Biol Chem* 2002; **277**: 38540–38549.
13 Zhu CH, Mouly V, Cooper RN, Mamchaoui K, Bigot A, Shay JW *et al.* Cellular senescence in human myoblasts is overcome by human telomerase reverse transcriptase and cyclin-dependent kinase 4: consequences in aging muscle and therapeutic strategies for muscular dystrophies. *Aging Cell* 2007; **6**: 515–523.
14 Cudre-Mauroux C, Occhiodoro T, Konig S, Salmon P, Bernheim L, Trono D. Lentivector-mediated transfer of Bmi-1 and telomerase in muscle satellite cells yields a Duchenne myoblast cell line with long-term genotypic and phenotypic stability. *Hum Gene Ther* 2003; **14**: 1525–1533.
15 Mukai A, Kurisaki T, Sato SB, Kobayashi T, Kondoh G, Hashimoto N. Dynamic clustering and dispersion of lipid rafts contribute to fusion competence of myogenic cells. *Exp Cell Res* 2009; **315**: 3052–3063.
16 Renault V, Thornell LE, Eriksson PO, Butler-Browne G, Mouly V. Regenerative potential of human skeletal muscle during aging. *Aging Cell* 2002; **1**: 132–139.
17 Sajko S, Kubinova L, Cvetko E, Kreft M, Wernig A, Erzen I. Frequency of M-cadherin-stained satellite cells declines in human muscles during aging. *J Histochem Cytochem* 2004; **52**: 179–185.
18 Wright WE, Shay JW. Historical claims and current interpretations of replicative aging. *Nat Biotechnol* 2002; **20**: 682–688.
19 Shay JW, Wright WE. Telomeres and telomerase: implications for cancer and aging. *Radiat Res* 2001; **155** (1 Part 2): 188–193.
20 Shay JW, Wright WE. Senescence and immortalization: role of telomeres and telomerase. *Carcinogenesis* 2005; **26**: 867–874.
21 Toussaint O, Medrano EE, von Zglinicki T. Cellular and molecular mechanisms of stress-induced premature senescence (SIPS) of human diploid fibroblasts and melanocytes. *Exp Gerontol* 2000; **35**: 927–945.
22 Haga K, Ohno S, Yugawa T, Narisawa-Saito M, Fujita M, Sakamoto M *et al.* Efficient immortalization of primary human cells by p16INK4a-specific short hairpin RNA or Bmi-1, combined with introduction of hTERT. *Cancer Sci* 2007; **98**: 147–154.
23 Bodnar AG, Ouellette M, Frolkis M, Holt SE, Chiu CP, Morin GB *et al.* Extension of life-span by introduction of telomerase into normal human cells. *Science* 1998; **279**: 349–352.
24 Ramirez RD, Sheridan S, Girard L, Sato M, Kim Y, Pollack J *et al.* Immortalization of human bronchial epithelial cells in the absence of viral oncoproteins. *Cancer Res* 2004; **64**: 9027–9034.
25 Ramirez RD, Morales CP, Herbert BS, Rohde JM, Passons C, Shay JW *et al.* Putative telomere-independent mechanisms of replicative aging reflect inadequate growth conditions. *Genes Dev* 2001; **15**: 398–403.
26 Carlson BM, Faulkner JA. Muscle transplantation between young and old rats: age of host determines recovery. *Am J Physiol* 1989; **256** (6 Part 1): C1262–C1266.
27 Benbassat CA, Maki KC, Unterman TG. Circulating levels of insulin-like growth factor (IGF) binding protein-1 and -3 in aging men: relationships to insulin, glucose, IGF, and dehydroepiandrosterone sulfate levels and anthropometric measures. *J Clin Endocrinol Metab* 1997; **82**: 1484–1491.
28 Doherty TJ, Vandervoort AA, Brown WF. Effects of ageing on the motor unit: a brief review. *Can J Appl Physiol* 1993; **18**: 331–358.
29 Rando TA, Blau HM. Primary mouse myoblast purification, characterization, and transplantation for cell-mediated gene therapy. *J Cell Biol* 1994; **125**: 1275–1287.
30 Decary S, Hamida CB, Mouly V, Barbet JP, Hentati F, Butler-Browne GS. Shorter telomeres in dystrophic muscle consistent with extensive regeneration in young children. *Neuromuscul Disord* 2000; **10**: 113–120.
31 Rao SS, Kohtz DS. Positive and negative regulation of D-type cyclin expression in skeletal myoblasts by basic fibroblast growth factor and transforming growth factor beta. A role for cyclin D1 in control of myoblast differentiation. *J Biol Chem* 1995; **270**: 4093–4100.
32 Guo K, Walsh K. Inhibition of myogenesis by multiple cyclin-Cdk complexes. Coordinate regulation of myogenesis and cell cycle activity at the level of E2F. *J Biol Chem* 1997; **272**: 791–797.
33 Hashimoto N, Ogashiwa M, Iwashita S. Role of tyrosine kinase in the regulation of myogenin expression. *Eur J Biochem* 1995; **227**: 379–387.
34 Hashimoto N, Ogashiwa M, Okumura E, Endo T, Iwashita S, Kishimoto T. Phosphorylation of a proline-directed kinase motif is responsible for structural changes in myogenin. *FEBS Lett* 1994; **352**: 236–242.
35 Sasaki R, Narisawa-Saito M, Yugawa T, Fujita M, Tashiro H, Katabuchi H *et al.* Oncogenic transformation of human ovarian surface epithelial cells with defined cellular oncogenes. *Carcinogenesis* 2009; **30**: 423–431.
36 Miyoshi H. Gene delivery to hematopoietic stem cells using lentiviral vectors. *Methods Mol Biol* 2004; **246**: 429–438.
37 Imabayashi H, Mori T, Gojo S, Kiyono T, Sugiyama T, Irie R *et al.* Redifferentiation of dedifferentiated chondrocytes and chondrogenesis of human bone marrow stromal cells via chondrosphere formation with expression profiling by large-scale cDNA analysis. *Exp Cell Res* 2003; **288**: 35–50.
38 Hirano H, Watanabe T. Microsequencing of proteins electrotransferred onto immobilizing matrices from polyacrylamide gel electrophoresis: application to an insoluble protein. *Electrophoresis* 1990; **11**: 573–580.
39 Bader D, Masaki T, Fischman DA. Immunochemical analysis of myosin heavy chain during avian myogenesis *in vivo* and *in vitro*. *J Cell Biol* 1982; **95**: 763–770.
40 Saito Y, Nonaka I, Qu Z, Balkir L, van Deutekom JC, Robbins PD *et al.* Initiation of satellite cell replication in bupivacaine-induced myonecrosis. *Acta Neuropathol (Berl)* 1994; **88**: 252–257.
41 Furukawa Y, Hashimoto N, Yamakuni T, Ishida Y, Kato C, Ogashiwa M *et al.* Down-regulation of an ankyrin repeat-containing protein, V-1, during skeletal muscle differentiation and its re-expression in the regenerative process of muscular dystrophy. *Neuromuscul Disord* 2003; **13**: 32–41.

Supplementary Information accompanies the paper on Gene Therapy website (http://www.nature.com/gt)

Geriatrics Gerontology INTERNATIONAL 1st Impact Factor in June 2010 Medline Indexed

Geriatr Gerontol Int 2011; **11:** *438–444*

ORIGINAL ARTICLE: EPIDEMIOLOGY, CLINICAL PRACTICE AND HEALTH

Association of polypharmacy with fall risk among geriatric outpatients

Taro Kojima,[1] Masahiro Akishita,[1] Tetsuro Nakamura,[2] Kazushi Nomura,[1] Sumito Ogawa,[1] Katsuya Iijima,[1] Masato Eto[1] and Yasuyoshi Ouchi[1]

[1]*Department of Geriatric Medicine, Graduate School of Medicine, University of Tokyo, and* [2]*Research Institute of Aging Science, Tokyo, Japan*

Aim: To investigate the association of fall risk with comorbidities and medications in geriatric outpatients in a cross-sectional design.

Methods: A total of 262 outpatients (84 men and 178 women, mean age 76.2 ± 6.8 years) were evaluated. Physical examination, clinical histories and medication profile were obtained from each patient. History of falls in the past year, 22-item fall risk index, 13-point simple screening test for fall, and time interval of one-leg standing test were examined as markers of fall risk.

Results: On univariate analysis, older age, female sex, hypertension, osteoporosis, history of stroke, number of comorbidities, use of antihypertensives, aspirin, bisphosphonates, hypnotics and number of prescribed drugs were significantly associated with either of four indices. On multiple regression analysis, the number of drugs was associated with all of the four indices, independent of other factors associated in the univariate analysis. The association of number of drugs with fall risk indices was stepwise.

Conclusion: In geriatric outpatients, polypharmacy rather than number of comorbidities was associated with fall risk. Prospective and intervention studies are needed to clarify the causal relationship between polypharmacy, comorbidities and fall risk. **Geriatr Gerontol Int 2011; 11: 438–444.**

Keywords: elderly, fall, polypharmacy, risk factors.

Introduction

Falls occur in more than 10% per year of community-dwelling elderly people,[1–3] and approximately 10% of falls lead to bone fracture. Also, falls are reported to be the third leading cause of a bedridden state among the elderly.[4] Previous studies assessed the risk factors of falls in community-dwelling elderly,[5–7] and history of falls, physical ability and living environment were found to be predictors of fall risk. However, these studies have not sufficiently assessed medical comorbidities and therapeutic drugs as risk factors of falls, although many elderly subjects have chronic illness such as hypertension, diabetes, cardiovascular diseases, osteoporosis and insomnia. Falls in patients on medications are more complicated, because some drugs such as aspirin could cause serious bleeding when they have injurious falls, and others such as antihypertensives[8] and hypoglycemic agents[9,10] could cause falls. Therefore, it is important to evaluate the association between fall risk and medical comorbidities or therapeutic drugs. Multiple drug use or polypharmacy is frequently seen in elderly patients because most of them have multiple chronic diseases to be treated. Moreover, inappropriate drug use is frequently seen in patients with polypharmacy.[11]

In Japan, a 22-item fall risk index questionnaire covering physical, cognitive, emotional and social aspects of

Accepted for publication 3 March 2011.

Correspondence: Dr Masahiro Akishita MD PhD, Department of Geriatric Medicine, Graduate School of Medicine, The University of Tokyo, 7-3-1 Hongo, Bunkyo-ku, Tokyo 113-8655, Japan. Email: akishita-tky@umin.ac.jp

 doi: 10.1111/j.1447-0594.2011.00703.x

functioning and environmental factors was established.[7] Also, by evaluating the validity of this questionnaire in community-dwelling older people, a simple screening test consisting of five items and total of 13 points was constructed.[2] Using these questionnaires and one-leg standing test[12] as indices of fall risk, we investigated the association of fall risk with comorbidities and medications in geriatric outpatients.

Methods

Patients

A total of 262 consecutive outpatients aged 65 years or older were enrolled who were referred for the treatment of chronic diseases such as hypertension, dyslipidemia, diabetes and osteoporosis every 2–4 weeks at a geriatric clinic located in Tokyo, Japan. All the patients were able to walk independently and were in stable conditions. Patients who had acute illness or overt dementia were excluded. Anthropometric and medical information were obtained including past history of stroke, myocardial infarction and malignancy. All the medical information including diagnoses and the prescribed drugs were obtained from the medical chart recorded by their physicians in charge. The patients whose prescriptions were changed within 1 month before enrollment were excluded. Accordingly, the included subjects had been taking the same drugs for at least 1 month before enrollment.

Ethical consideration

This study was approved by the Institutional Review Board of the Research Institute of Aging Science. We obtained written consent from all participants and/or their guardians.

Four indices of fall tendency

On the day of the enrollment, all patients were examined for four indices to investigate the fall risk: (i) history of fall in the past year (no or yes); (ii) a 22-item portable fall risk index questionnaire developed by the working group of the Ministry of Health, Labor and Welfare (see Appendix I);[7] (iii) 13-point simple screening test to assess the risk of fall which was also developed by the same working group (see Appendix II);[2] and (iv) duration time of open-eye one-leg standing test.

Table 1 Characteristics of study subjects

Age			76.2 ± 6.8 years old
Male	32.1%	(n = 84)	75.3 ± 6.6 years old
Female	67.9%	(n = 178)	76.6 ± 6.8 years old
Comorbidities			
Hypertension	64.1%	(n = 168)	
Dyslipidemia	47.7%	(n = 125)	
Diabetes	18.7%	(n = 49)	
Osteoporosis	24.0%	(n = 63)	
History of stroke	6.5%	(n = 17)	
History of myocardial infarction	3.4%	(n = 9)	
History of cancer	5.3%	(n = 14)	
Number of comorbidities	1.90 ± 1.09		
Drug use			
Antihypertensive use	57.6%	(n = 151)	
Calcium channel blockers	39.3%	(n = 103)	
Angiotensin-II receptors blockers	34.7%	(n = 91)	
Beta-blocker	6.9%	(n = 18)	
Angiotensin converting enzyme inhibitors	5.7%	(n = 15)	
Diuretics	5.0%	(n = 13)	
Statins	24.4%	(n = 64)	
Sulfonylureas	6.5%	(n = 17)	
Aspirin	20.6%	(n = 54)	
Vitamin D	4.6%	(n = 12)	
Bisphosphonates	6.5%	(n = 17)	
H_2-blockers	9.9%	(n = 26)	
Proton pump inhibitors	6.5%	(n = 17)	
Hypnotics	18.3%	(n = 48)	
Number of drugs	3.4 ± 2.8		

Values are expressed as mean ± standard deviation.

Experience of falls in the past year is an established and powerful tool for assessing fall risk,[2] and was reported by the patient and/or his or her family members. Duration time of one-leg standing test, which can be carried out in a narrow limited space of the outpatient office, was measured using the leg with the eyes open, until the raised leg was put down on the floor. We examined both right and left legs once for each, and the longer of the two measurements was used for statistical analysis.[12]

Data analysis and statistical methods

Values are expressed as means ± standard deviation. In order to analyze the relationship between each fall risk index and comorbidities or drugs, variables were compared using Student's *t*-test or the χ^2-test as appropriate. The correlations between the two continuous variables were analyzed using Pearson's *r* coefficient. In multivariate analysis, logistic regression analysis was performed for history of falls and multiple regression analysis for the remaining three indices, to determine the association of fall risk with the variables. Differences between the groups of number of drugs and three indices of fall tendency were analyzed using one-factor ANOVA followed by Tukey–Kramer test. Data were analyzed using JMP version 8.0.1.

Results

The characteristics of the study subjects are shown in Table 1. Calcium channel blockers, angiotensin-II receptor blockers (ARB), statins and aspirins were prescribed in more than 20% of all the patients. Calcium channel blockers prescribed in this study were all long-acting agents, and aspirin dosage prescribed were all 100 mg. Less than 10 patients received insulin therapy, took non-steroidal anti-inflammatory drugs or anticoagulants. No patients were taking neuroleptics, nor antiparkinsonian drugs. Patients prescribed five drugs or more were 36.3%.

On univariate analyses, the number of drugs was the only factor which was significantly associated with history of falls in the past year (no/yes 3.2 ± 2.6/4.0 ± 3.1 drugs, $P < 0.05$). Older age, female, hypertension, osteoporosis, history of stroke, the number of comorbidities, use of ARB, aspirin, bisphosphonates, hypnotics and number of prescribed drugs were significantly associated with either one of three indices of fall risk (Table 2). Number of drugs was significantly correlated with three scores excluding the

Table 2 Univariate analysis of association between risk factor variables and three fall indices: fall-predicting score, simple screening test, one-leg standing test

		Fall risk index (points)	Simple screening test (points)	One-leg standing test (seconds)
Age		0.23***	0.23***	−0.46***
Female	No/Yes	7.0 ± 3.1/8.4 ± 4.0**	3.8 ± 3.3/4.7 ± 3.6*	19.7 ± 11.7/16.2 ± 11.7*
Hypertension	No/Yes	7.2 ± 3.6/8.4 ± 3.8*	3.7 ± 3.3/4.8 ± 3.5*	18.9 ± 11.1/16.2 ± 12.1
Osteoporosis	No/Yes	7.6 ± 3.7/8.9 ± 4.0*	4.3 ± 3.6/4.8 ± 3.1	17.9 ± 11.7/15.6 ± 11.9
History of stroke	No/Yes	7.8 ± 3.7/9.7 ± 4.1*	4.3 ± 3.4/5.6 ± 4.1	17.9 ± 11.8/8.5 ± 8.7**
Number of comorbidies		0.27***	0.17*	−0.24***
Antihypertensives	No/Yes	7.3 ± 3.6/8.5 ± 3.8*	3.7 ± 3.3/4.9 ± 3.5*	18.8 ± 11.4/15.9 ± 12.0
Angiotensin-II receptor blockers	No/Yes	7.6 ± 3.7/8.7 ± 3.8*	3.9 ± 3.4/5.2 ± 3.5**	17.6 ± 11.5/16.3 ± 12.2
Calcium channel blockers	No/Yes	7.6 ± 3.7/8.5 ± 3.7	4.1 ± 3.5/4.8 ± 3.5	18.8 ± 11.6/14.3 ± 11.6**
Aspirin	No/Yes	7.7 ± 3.8/8.9 ± 3.8*	4.1 ± 3.5/5.5 ± 3.7*	18.0 ± 11.8/13.5 ± 11.5*
Bisphosphonates	No/Yes	7.8 ± 3.8/9.9 ± 2.5*	4.3 ± 3.5/6.5 ± 2.7*	17.3 ± 11.8/14.9 ± 11.7
Hypnotics	No/Yes	7.6 ± 3.6/9.7 ± 4.1***	4.2 ± 3.6/5.2 ± 3.1	17.6 ± 11.9/15.2 ± 11.3
Number of drugs		0.30***†	0.27***†	−0.35***

*$P < 0.05$; **$P < 0.005$; ***$P < 0.0005$, compared to "No" by simple Student's *t*-test. For age, number of comorbidities and number of drugs, Pearson's correlation coefficient between each indices of fall tendency are shown. †For analysis of number of drugs, a questionnaire asking "whether taking five or more drugs" were excluded for analysis. Therefore, fall risk index was analyzed by a total of 21 items, and a simple screening test by a total of 11 points. For other risk factor variables shown in the table, mean ± standard deviations are expressed. Other risk factor variables not shown in this table showed no statistically significant relationship with either one of three indices.

[Table 2 amended after online publication date September 27, 2011]

question on polypharmacy. Number of comorbidities was significantly associated with age ($r = 0.32$, $P < 0.0001$) and with the number of drugs ($r = 0.62$, $P < 0.0001$).

Next, on multivariate analyses, the questionnaire asking "whether taking five or more drugs" were excluded from the fall risk index and the simple screening test. Therefore, the fall risk index was analyzed by a total of 21 items and the simple screening test by a total of 11 points in this analysis. To evaluate the association of four fall risk indices with comorbidities and drugs, all the variables that were significantly associated in either one of four univariate analyses were entered into the model. As shown in Table 3, the number of drugs was the only factor which was significantly associated with all four indices, independent of age, sex and other variables. Because each disease variable or drug variable might have affected the number of comorbidities or the number of drugs in this analysis, we just compared the number of comorbidities and the number of drugs to exclude the double count in next analysis. As shown in Table 4, the number of drugs was significantly associated with all of the four fall risk indices independent of age, sex and the number of comorbidities, while the number of comorbidies was inversely associated with history of falls and simple screening test. As shown in Figure 1, the association of the number of drugs with

Table 3 Multivariate analysis of association between risk factor variables and four fall indices: history of falls in a year, fall risk index, simple screening test, one leg standing test

		History of fall in a year (No = 0/Yes = 1) Odds ratio (95% CI)	Fall risk index (21 items)† β	Simple screening test (11 points)† β	One-leg standing test (s) β
Age		1.00 (0.96–1.05)	0.073	0.127	–0.370***
Female	(No = 0/Yes = 1)	2.36 (1.12–5.00)*	0.199**	0.197**	–0.149*
Hypertension	(No = 0/Yes = 1)	1.87 (0.61–5.76)	0.166	0.218*	–0.110
Osteoporosis	(No = 0/Yes = 1)	0.67 (0.28–1.60)	0.093	0.027	0.023
History of stroke	(No = 0/Yes = 1)	1.43 (0.38–5.45)	0.080	0.032	–0.083
Number of comorbities		0.60 (0.38–0.95)*	–0.062	–0.237*	–0.024
Antihypertensives					
	(No = 0/Yes = 1)	0.52 (0.18–1.54)	–0.141	–0.158	0.142
Aspirin	(No = 0/Yes = 1)	1.59 (0.72–3.50)	0.053	0.046	0.002
Bisphosphonates	(No = 0/Yes = 1)	2.27 (0.73–7.07)	0.055	0.105	0.033
Hypnotics	(No = 0/Yes = 1)	0.84 (0.33–2.15)	0.094	–0.018	0.084
Number of drugs		1.24 (1.07–1.45)*	0.247**	0.335***	–0.250**

*$P < 0.05$; **$P < 0.005$; ***$P < 0.0005$. Logistic regression analysis was performed for history of fall in a year, and multiple regression analysis for the remaining three. The risk factor variables used in these multivariate analyses were those associated in either of the four univariate analysis significantly. †The questionnaire asking "whether taking five or more drugs" were excluded from the scores in this analysis. Therefore, fall risk index were analyzed by a total of 21 items and simple screening test by a total of 11 points. CI, confidence interval; β, standardized regression coefficient.
[Table 3 amended after online publication date September 27, 2011]

Table 4 Multivariate analysis of association between number of comorbidities and drugs with four fall indices: history of falls in a year, fall risk index, simple screening test, one-leg standing test

	History of fall in a year (No = 0/Yes = 1) Odds ratio (95% CI)	Fall-risk index (21 items)† β	Simple screening test (11 points)† β	One-leg standing test (s) β
Age	1.00 (0.96–1.05)	0.101	0.115	–0.376***
Female (No = 0/Yes = 1)	1.73 (0.90–3.34)	0.207**	0.191**	–0.110
Number of comorbidities	0.63 (0.45–0.89)*	0.073	–0.137	–0.034
Number of drugs	1.23 (1.08–1.41)*	0.223*	0.316***	–0.233**

*$P < 0.05$; **$P < 0.005$; ***$P < 0.0005$. Logistic regression analysis was performed for history of fall in a year, and multiple regression analysis for the remaining three. †The questionnaire asking "whether taking five or more drugs" were excluded from the scores in this analysis. Therefore, fall risk index was analyzed by a total of 21 items and simple screening test by a total of 11 points. CI, confidence interval; β, standardized regression coefficient.

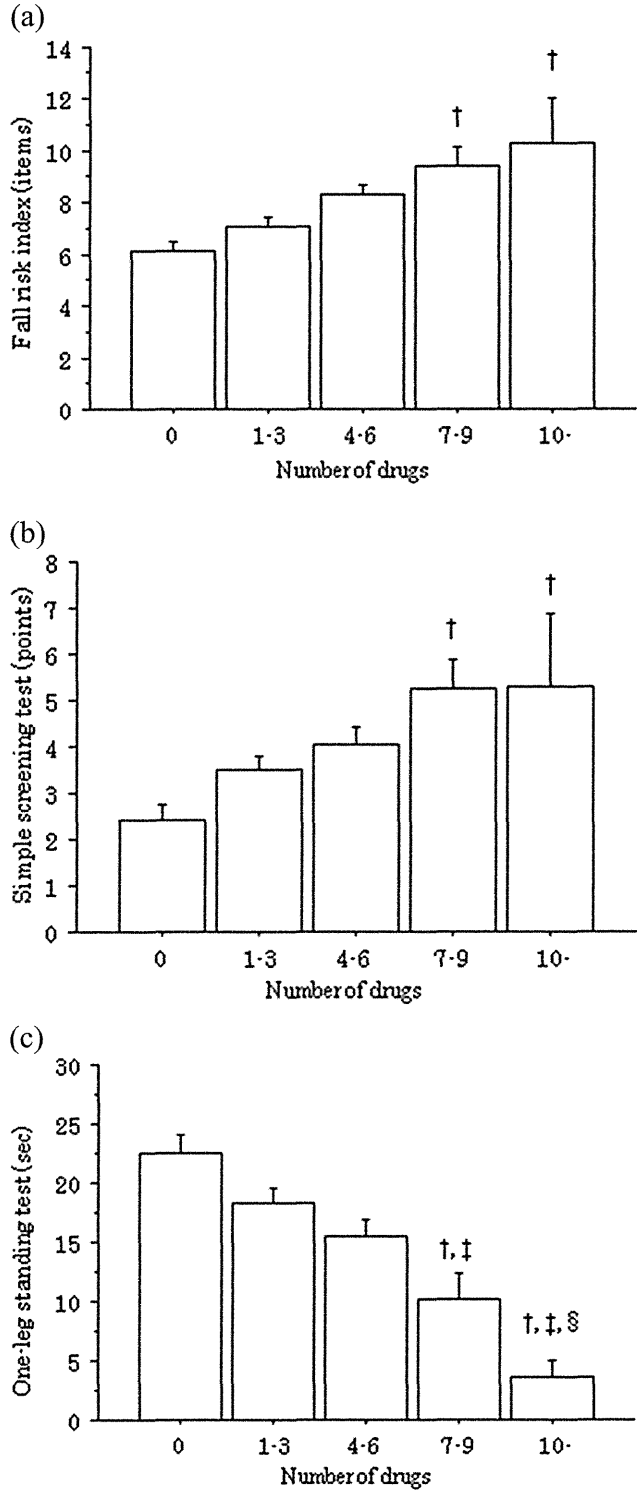

Figure 1 Averages of fall risk according to the number of drugs. (a) Fall risk index excluding the questionnaire concerning polypharmacy. (b) Simple screening test excluding the questionnaire concerning polypharmacy. (c) Duration time of one-leg standing test. The differences between the number of the drugs were compared through ANOVA, $P < 0.0001$ for (a), $P < 0.005$ for (b), $P < 0.0001$ for (c). For post-hoc analysis, $^{\dagger}P < 0.05$ vs 0 drug; $^{\ddagger}P < 0.05$ vs 1–3 drugs; $^{\S}P < 0.05$ vs 4–6 drugs. Values are expressed as mean ± standard error.

fall predicting score, simple screening test and duration time of one-leg standing test was stepwise.

Discussion

Epidemiological studies have assessed the risk of falls in community-dwelling people, but not in geriatric outpatients, who are likely to fall and need special consideration for the treatment of their illness. This cross-sectional study investigated the association between comorbidities, medications and fall risks in Japanese elderly outpatients and found that all four indices were significantly associated with the number of drugs. Because polypharmacy is frequently seen in patients with multiple comorbidities, this study compared the impact of the number of drugs with that of the number of comorbidities on fall risk, and found the significance of polypharmacy as fall risk in elderly outpatients.

In the present study, the number of comorbidities was inversely associated with the history of fall in the past year and with an 11-point simple screening test in the multivariate analysis. The reason is unclear; however, there are some speculations about this. None of the patients with four or more comorbidities ($n = 19$, 79.4 ± 5.2 years old) had history of fall in the past year. This accounts for the lower points of the simple screening test in these patients, because the history of fall consists of 5 points out of a total of 11 points in the simple screening test. So the question is why they had lower frequency of falling experiences, although they are at higher risk of falls according to fall risk index and one-leg standing test (9.6 ± 3.8 items and 8.6 ± 9.4 s, respectively). These patients may take care not to fall in their daily lives because of their consciousness of fall risk or frailty, or maybe due to elevated vigilance of caregivers and their constant physical assistances. They might have simply forgotten their fall experiences due to subclinical cognitive impairment, although demented patients were not included in this study. It is also possible that the patients who had more comorbidities and had fallen did not meet our inclusion criteria because of their recent injurious falls or their severe conditions.

Several medications and comorbidities have been reported as risks of fall.[6,7,13–19] Among these, diabetes,[9,10] imsonia,[13] hypnotics[13–15] and antihypertensive use[8] were not significantly associated with fall risk in our study. Only 20 patients (40.8% of diabetic patients) were prescribed hypoglycemic agents such as sulfonylurea ($n = 17$) or insulin ($n = 3$) in this study. Because hypoglycemia is considered to be the main cause of accidental falls in diabetic patients, relatively less prescription of hypoglycemic agents might have affected our result. The patients who were prescribed hypnotics tended to be at higher risk of falls in univariate analysis, which did show statistical significance. Also, antihypertensives such as diuretics are reported to increase the fall risk.[8] No

association between these drugs and fall risk in our study might be due to the small sample size. Other drugs such as major tranquillizers,[14] antidepressants[17,18] and antiparkinsonians[19] might increase fall risk; however, very few patients used these drugs in this study.

There are some other limitations. First, the causal relationship of the associations observed in this study is unknown because of the cross-sectional design. Polypharmacy has been regarded as a risk in several aspects in elderly patients. Previous studies have shown that adverse drug events were seen more frequently in the polypharmacy patients during their stay in the geriatric inpatient ward,[20] and polypharmacy was one of the important predictors for postdischarge mortality in elderly patients after emergent hospitalization.[21] Because patients with multiple diseases and in severer conditions are likely to take more medications, we used the number of comorbidities in analysis as fall risk variables. However, it is still unclear whether polypharmacy is a risk of falls independent of severity of each comorbidity. Interventional studies to reduce the number of drugs are needed to clarify the causal relationship between polypharmacy and fall risk. Second, this study did not evaluate the fall itself. The validity of four indices used in this study is well established as fall risk markers. However, prospective studies which evaluate the incidence of fall should be carried out in the future. Third, although the included subjects were receiving the same prescriptions for more than 1 month, the exact duration of each drug use or polypharmacy was not assessed in this study. Consequently, the long-term adverse effects over months or years seen in elderly patients should be more precisely investigated.

In summary, this study demonstrated that geriatric outpatients with polypharmacy were at higher risk of falls, consistent with the previous studies conducted in community-dwelling elderly. Our finding may add new information on pharmacotherapy in elderly patients with chronic diseases. Prospective studies and intervention studies examining the effect of drug reduction are needed in the future.

Acknowledgments

We thank Ms Fumie Tanaka for her excellent technical assistance. This study was financially supported by a grant from the Ministry of Health, Labor and Welfare in Japan (H21-Chouju-Ippan-005, H22-Chouju-Shitei-009).

References

1 Wada T, Ishine M, Ishimoto Y *et al.* Community-dwelling elderly fallers in Japan are older, more disabled, and more depressed than nonfallers. *J Am Geriatr Soc* 2008; **56**: 1570–1571.
2 Okochi J, Toba T, Takahashi T *et al.* Simple screening test for risk of falls in the elderly. *Geriatr Gerontol Int* 2006; **6**: 223–227.
3 Rubenstein LZ. Falls in older people: epidemiology, risk factors and strategies for prevention. *Age Ageing* 2006; **35–52** (Suppl 2): ii37–ii41.
4 Aoyagi K, Ross PD, Davis JW, Wasnich RD, Hayashi T, Takemoto T. Falls among community-dwelling elderly in Japan. *J Bone Miner Res* 1998; **13**: 1468–1474.
5 Stel VS, Pluijm SM, Deeg DJ, Smit JH, Bouter LM, Lips P. A classification tree for predicting recurrent falling in community-dwelling older persons. *J Am Geriatr Soc* 2003; **51**: 1356–1364.
6 Kojima S, Furuna T, Ikeda N, Nakamura M, Sawada Y. Falls among community-dwelling elderly people of Hokkaido, Japan. *Geriatr Gerontol Int* 2008; **8**: 272–277.
7 Toba K, Okochi J, Takahashi T *et al.* Development of a portable fall risk index for elderly people living in the community. *Nippon Ronen Igakkai Zasshi* 2005; **42**: 346–352. (In Japanese).
8 Leipzig RM, Cumming RG, Tinetti ME. Drugs and falls in older people: a systematic review and meta-analysis: II. Cardiac and analgesic drugs. *J Am Geriatr Soc* 1999; **47**: 40–50.
9 Berlie HD, Garwood CL. Diabetes medications related to an increased risk of falls and fall-related morbidity in the elderly. *Ann Pharmacother* 2010; **44**: 712–717.
10 Araki A, Ito H. Diabetes mellitus and geriatric syndromes. *Geriatr Gerontol Int* 2009; **9**: 105–114.
11 Akishita M, Arai H, Arai H *et al.* Survey on geriatricians' experiences of adverse drug reactions caused by potentially inappropriate medications: Commission report of the Japan Geriatrics Society. *Geriatr Gerontol Int* 2011; **11**: 3–7.
12 Michikawa T, Nishiwaki Y, Takebayashi T, Toyama Y. One-leg standing test for elderly populations. *J Orthop Sci* 2009; **14**: 675–685.
13 Ensrud KE, Blackwell TL, Redline S *et al.* Sleep disturbances and frailty status in older community-dwelling men. *J Am Geriatr Soc* 2009; **57**: 2085–2093.
14 Leipzig RM, Cumming RG, Tinetti ME. Drugs and falls in older people: a systematic review and meta-analysis: I. Psychotropic drugs. *J Am Geriatr Soc* 1999; **47**: 30–39.
15 Woolcott JC, Richardson KJ, Wiens MO *et al.* Meta-analysis of the impact of 9 medication classes on falls in elderly persons. *Arch Intern Med* 2009; **169**: 1952–1960.
16 Tinetti ME, Speechley M, Ginter SF. Risk factors for falls among elderly persons living in the community. *N Engl J Med* 1988; **319**: 1701–1707.
17 Kelly KD, Pickett W, Yiannakoulias N *et al.* Medication use and falls in community-dwelling older persons. *Age Ageing* 2003; **32**: 503–509.
18 Thapa PB, Gideon P, Cost TW, Milam AB, Ray WA. Antidepressants and the risk of falls among nursing home residents. *N Engl J Med* 1998; **339**: 875–882.
19 Bloem BR, Steijns JA, Smits-Engelsman BC. An update on falls. *Curr Opin Neurol* 2003; **16**: 15–26.
20 Arai H, Akishita M, Teramoto S *et al.* Incidence of adverse drug reactions in geriatric units of university hospitals. *Geriatr Gerontol Int* 2005; **5**: 293–297.
21 Iwata M, Kuzuya M, Kitagawa Y, Suzuki Y, Iguchi A. Underappreciated predictors for postdischarge mortality in acute hospitalized oldest-old patients. *Gerontology* 2006; **52**: 92–98.

Appendix I. 22 items of fall-predicting score (questionnaire)

Q1. Have you fallen during the last 12 months?	Yes, 1; No, 0.
Q2. Have you tripped during the last 12 months?	Yes, 1; No, 0.
Q3. Can you climb stairs without help?	Yes, 0; No, 1.
Q4. Do you feel your walking speed has declined recently?	Yes, 1; No, 0.
Q5. Can you cross a road within the green signal interval?	Yes, 0; No, 1.
Q6. Can you walk 1 km without stopping?	Yes, 0; No, 1.
Q7. Can you stand on one foot for about five seconds?	Yes, 0; No, 1.
Q8. Do you use a stick when you walk?	Yes, 1; No, 0.
Q9. Can you squeeze a towel tightly?	Yes, 0; No, 1.
Q10. Do you feel dizzy at times?	Yes, 1; No, 0.
Q11. Is your back bent?	Yes, 1; No, 0.
Q12. Do you have knee pain?	Yes, 1; No, 0.
Q13. Do you have a problem with your vision?	Yes, 1; No, 0.
Q14. Do you have a hearing problem?	Yes, 1; No, 0.
Q15. Do you think you are forgetful?	Yes, 1; No, 0.
Q16. Do you feel anxious about falling when you walk?	Yes, 1; No, 0.
Q17. Do you take five or more prescribed medicines?	Yes, 1; No, 0.
Q18. Do you feel unsafe because your home is dark?	Yes, 1; No, 0.
Q19. Are there any obstacles in your house?	Yes, 1; No, 0.
Q20. Is there any difference in level within your home?	Yes, 1; No, 0.
Q21. Do you have to use stairs in daily living?	Yes, 1; No, 0.
Q22. Do you have to walk on a steep slope around your house?	Yes, 1; No, 0.

Appendix II. Simple screening test for risk of falls

Q1. Have you fallen during the last 12 months?	Yes, 5 points; No, 0.
Q2. Do you feel your walking speed has declined recently?	Yes, 2 points; No, 0.
Q3. Do you use a cane when you walk?	Yes, 2 points; No, 0.
Q4. Is your back bent?	Yes, 2 points; No, 0.
Q5. Do you take five or more prescribed medicines?	Yes, 2 points; No, 0.

Sirtuin 1 Retards Hyperphosphatemia-Induced Calcification of Vascular Smooth Muscle Cells

Aya Takemura, Katsuya Iijima, Hidetaka Ota, Bo-Kyung Son, Yuki Ito, Sumito Ogawa, Masato Eto, Masahiro Akishita, Yasuyoshi Ouchi

Objective—Arterial calcification is associated with cardiovascular disease as a complication of advanced atherosclerosis. Aged vascular cells manifest some morphological features of a senescent phenotype. Recent studies have demonstrated that mammalian sirtuin 1 (SIRT1), a histone deacetylase, is an exciting target for cardiovascular disease management. Here, we investigated the role of SIRT1 in a calcification model of vascular smooth muscle cells (SMCs).

Methods and Results—In adenine-induced renal failure rats with hyperphosphatemia, massive calcification was induced in the aortic media. Senescence-associated β-galactosidase (SAβ-gal) activity, a marker of cellular senescence, in medial SMCs was significantly increased, and its induction was positively associated with the degree of calcification. In cultured SMCs, inorganic phosphate (Pi) stimulation dose-dependently increased SAβ-gal-positive cells, and Pi-induced senescence was associated with downregulation of SIRT1 expression, leading to p21 activation. The activation via SIRT1 downregulation was blunted by inhibition of Pi cotransporter. Activation of SIRT1 by resveratrol significantly reduced the senescence-associated calcification. Conversely, SIRT1 knockdown by small interfering RNA accelerated the Pi-induced SMC senescence and subsequent calcification. In addition, SIRT1 knockdown induced phenotypic change from a differentiated state to osteoblast-like cells. The senescence-related SMC calcification was completely prevented by p21 knockdown. In addition to Pi-induced premature senescence, SMCs with replicative senescence were also more sensitive to Pi-induced calcification compared with young SMCs, and this finding was attributable to augmented p21 expression.

Conclusion—SIRT1 plays an essential role in preventing hyperphosphatemia-induced arterial calcification via inhibition of osteoblastic transdifferentiation. In addition, Pi-induced SMC calcification may be associated with both premature and replicative cellular senescence. (***Arterioscler Thromb Vasc Biol.* 2011;31:2054-2062.)**

Key Words: cellular senescence ■ hyperphosphatemia ■ longevity gene SIRT1 ■ vascular calcification ■ vascular smooth muscle cell

Atherosclerotic vascular damage associated with aging manifests several features, namely atherosis, sclerosis, and calcific change, finally leading to cardiovascular events. These pathological changes result in arterial wall thickening (localized morphological changes) and arterial stiffening (functional changes).[1] Arterial calcification makes the management of hemodynamics more difficult in the elderly, because ectopic calcium deposition in the aorta and arteries contributes to vessel wall stiffening and loss of elastic recoil.[2] These pathological conditions result in unstable hemodynamic consequences, finally leading to a decline in end-organ perfusion and subsequent ischemic events. Recently, several reports have demonstrated that aortic calcification detectable on chest X-ray examination is a strong predictor of future cardiovascular events beyond traditional risk factors.[3]

Arterial calcification is anatomically separated into two types, intimal and medial calcification.[4] Intimal calcification, which is seen as patchy scattered deposits only occurring within atherosclerotic plaques, is shown to be associated with plaque vulnerability.[5] On the other hand, medial calcification, which is frequently seen in the elderly and in diabetes and chronic renal failure, is observed as continuous linear deposits along the internal elastic lamina.[6] Advanced atherosclerosis with both types of calcified lesions is the consequence of overlapping pathological mechanisms.

Ectopic calcification in the vasculature has been shown to result from passive precipitation of calcium with aging and osteoporosis, the so-called calcium shift theory, as a previous hypothesis.[7] However, accumulating recent evidence has shown it to be attributable to an active "cell-mediated process" resembling osteogenesis in bone rather than passive mineral precipitation in vascular smooth muscle cells (SMCs).[8,9]

Silent information regulator-2 (Sir2), an NAD^+-dependent HDAC, is highly conserved in organisms ranging from Archaea

Received on: May 12, 2010; final version accepted on: May 25, 2011.

From the Department of Geriatric Medicine, Graduate School of Medicine, University of Tokyo, Tokyo, Japan.

Correspondence to Katsuya Iijima, MD, PhD, Department of Geriatric Medicine, Graduate School of Medicine, University of Tokyo, 7-3-1 Hongo, Bunkyo-ku, Tokyo 113-8655, Japan. E-mail katsu-tky@umin.ac.jp

Arterioscler Thromb Vasc Biol **is available at http://atvb.ahajournals.org** **DOI: 10.1161/ATVBAHA.110.216739**

to humans.[10] In yeast, Sir2 has been shown to play critical roles in DNA repair, stress resistance, and longevity. Mammalian sirtuin 1 (SIRT1), the closest homolog of Sir2, regulates the cell cycle, apoptosis, and metabolism by interacting with a number of molecules, including p53, promyelocytic leukemia protein, Foxo, Ku70, and peroxisome proliferator-activated receptor-γ.[11] A previous study has shown that SIRT1 antagonizes p53-mediated premature senescence in mouse embryo fibroblasts.[12] In addition, we have recently demonstrated that SIRT1 inhibits oxidative stress-induced premature senescence in vascular endothelial cells.[13] However, the detailed mechanism of how SIRT1 affects vascular SMC senescence and arterial calcification remains unclear.

In this study, we hypothesized that SIRT1 plays an important role in preventing arterial calcification due to renal failure, in association with modulation of cellular senescence. Here, we demonstrated the protective potential of SIRT1 against hyperphosphatemia-induced premature and replicative senescence and subsequent calcification in SMCs.

Methods

Aortic Calcification in Renal Failure Rats

Renal failure was induced in rats by a 0.75% adenine-containing diet as previously described.[14] All procedures and animal care were in accordance with the Guide for the Care and Use of Laboratory Animals of the University of Tokyo. Detailed methods are described in the supplemental materials, available online at http://atvb.ahajournals.org.

Induction of SMC Calcification

Primary human aortic SMCs (HASMCs) were treated with a pathological concentration of inorganic phosphate (Pi) up to 3.2 mmol/L in culture medium as previously described.[29] To quantitatively measure Pi-induced calcification, two distinct experiments were performed as previously described[14]: (1) intracellular calcium deposition as determined by *o*-cresolphthalein complexone method, and (2) visualization of mineralization as determined by von Kossa staining, Detailed methods are described in the supplemental materials.

Senescence-Associated β-Galactosidase Staining

To assess senescent changes in the phenotype of cultured HASMCs or aortic medial cells of rats, staining for senescence-associated β-galactosidase (SAβ-gal), a well-established biomarker of cellular senescence, was performed. Detailed methods are described in the supplemental materials.

Knockdown of SIRT1 or p21 by Small Interfering RNA

HASMCs were transfected with 200 pmol/L small interfering RNA (siRNA) for SIRT1, $p21^{WAF1/CIP1}$, or both. Detailed methods are described in the supplemental materials.

Real-Time Polymerase Chain Reaction Analysis: Osteoblastic Markers

To examine whether Pi stimulation induces change to an osteoblastic phenotype, the expression of Runx-2/Cbfa-1 and alkaline phosphatase, which are well known to be representative osteoblastic markers, was checked using real time-polymerase chain reaction analysis. In addition, the effect of knockdown of SIRT1, p21, or both by siRNA on the osteoblastic phenotypic change in HASMCs was examined. Primer sequences are shown in Supplemental Figure I.

Results

Association of Senescent Vascular Cells With Aortic Medial Calcification in Renal Failure Rats

The adenine-fed rats had severe renal failure, with a huge increase in serum creatinine (3.0±0.9 mg/dL in renal failure rats versus 0.3±0.0 mg/dL in control rats), similar to a previous report.[14] The renal failure rats showed an approximately 2.0-fold increase in serum phosphorus (18.9±4.7 mg/dL) compared with control rats (9.8±0.9 mg/dL). Histological assessment using von Kossa staining showed that the aorta in renal failure rats had extensive linear calcification, which was localized in the aortic media, resembling the typical Mönckeberg's pattern (Figure 1A). Numerous SAβ-gal positive cells were found in the aortic media of renal failure rats, whereas the aortic wall in control rats did not contain senescent cells (Figure 1B). The senescent cells were mainly localized to the calcified area and its surrounding area, which was defined as the area not stained black by von Kossa staining. Quantitative assessment showed that the number of senescent cells with high SAβ-gal activity was positively correlated with the calcified area in the aortic media (Figure 1C).

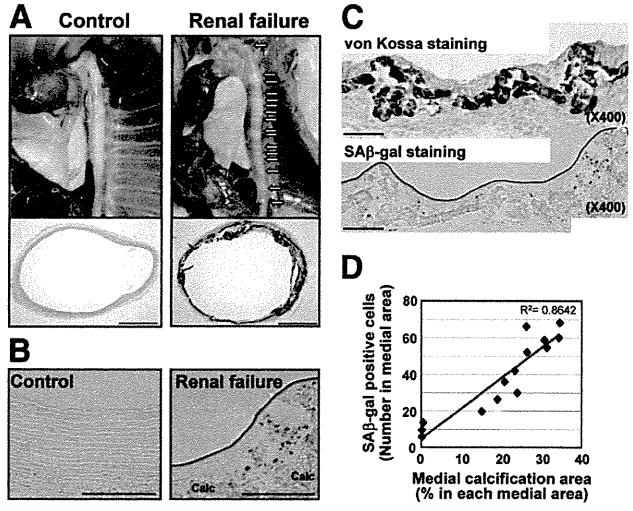

Figure 1. Presence of senescent vascular cells colocalized with calcification in aortic media of renal failure rats. A, Rats with severe renal failure had massive calcification throughout the aorta (right) compared with control rats (left) (n=5). Yellow arrows indicate calcified area. Morphological assessment by von Kossa staining showed extensive calcification in the aortic media of renal failure rats. Scale bar=500 μm. B, Senescent vascular cells (senescence-associated β-galactosidase [SAβ-gal]-positive: blue) were significantly detected throughout the calcified area (Calc) in renal failure rats, whereas these senescent cells were not present in control rats. Scale bar=100 μm. C, Localized association between calcification and senescent cells is shown in renal failure rats. SAβ-gal-positive cells were frequently found in areas with marked calcification. D, The association of the number of SAβ-gal-positive cells with the calcified area in each photograph was evaluated. The senescent cell number was linearly correlated with the area of calcification in the aortic media of renal failure rats (calcified area in media: percentage).

Pi Induces Cellular Senescence in Cultured SMCs

On the basis of our results obtained from animal experiments, we hypothesized that senescent SMCs in the aortic media are strongly associated with the development of arterial calcification. Therefore, the effect of excessive Pi stimulation (2.6 mmol/L) on cellular senescence in cultured SMCs was examined. SAβ-gal-positive senescent HASMCs were significantly induced by not only angiotensin II (Ang II) but also Pi

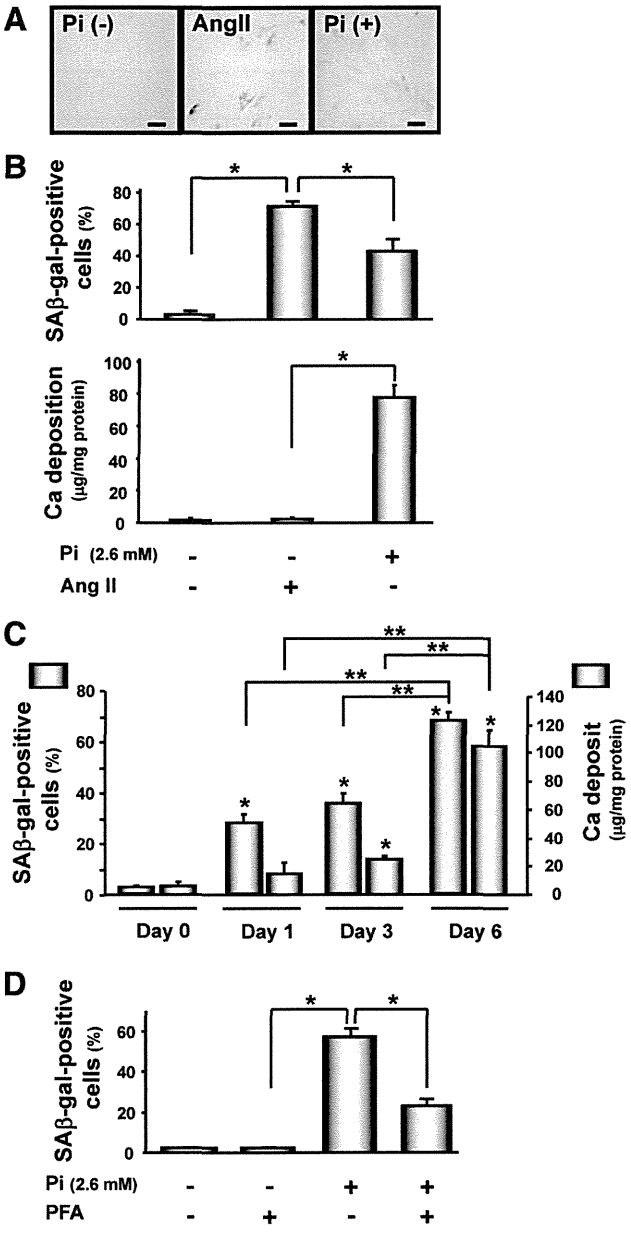

Figure 2. Inorganic phosphate (Pi) stimulation induces cellular senescence in vascular smooth muscle cells (SMCs) via its cotransporter. A, The effect of Pi on senescent transition in human aortic SMCs (HASMCs) was examined. Representative photographs showed that senescence-associated β-galactosidase (SAβ-gal) activity (blue) in cells was significantly induced by not only angiotensin II (Ang II: 10 pmol/L, as a positive control) but also Pi stimulation (2.6 mmol/L). B, The number of senescent cells was significantly increased by not only Ang II but also Pi. Calcium deposition was significantly increased by Pi; however, calcification in HASMCs was not induced by Ang II alone in the absence of Pi. C, Senescent cells were significantly increased by Pi stimulation even on day 1; however, a statistically significant increase in calcium deposition was found from day 3 and later. D, Inhibition of the phosphate cotransporter Na-dependent phosphate cotransporter by the inhibitor phosphonoformic acid (PFA) (100 μmol/L) reduced SAβ-gal activity, which was increased by Pi (2.6 mmol/L) in HASMCs. Each experiment was performed al least 3 times.

stimulation (Figure 2A). Notably, Pi stimulation increased calcium deposition; however, Ang II alone did not (Figure 2B). It suggests that high-dose Pi condition, but not stress by Ang II alone, is indispensable to induce SMC calcification. These findings also suggest that intracellular Pi influx at least is essential to induce this SMC calcification model.

In addition, to determine how many days after the initiation of Pi stimulation the cells showed a senescent phenotype and subsequent calcification, the time-dependent effects of Pi stimulation on both SAβ-gal activity and calcium deposition were examined. As shown in Figure 2C, SAβ-gal-positive cells were significantly increased by Pi stimulation even on day 1, although calcium deposition was not markedly increased at the same time point. A statistically significant increase in calcium deposition was found from day 3 and later. Cotreatment with phosphonoformic acid, an inhibitor of Na-dependent phosphate cotransporter (NPC), showed significant inhibition of Pi-induced senescence (Figure 2D). Our previous report showed that treatment with PFA completely inhibited Pi-induced SMC calcification,[15] suggesting the importance of increased intracellular influx of phosphate in Pi-induced SMC senescence.

Downregulation of SIRT1 by Pi

Treatment of HASMCs with Pi caused downregulation of SIRT1 expression in a time-dependent manner (Figure 3A). The decline was dependent on Pi concentration (data not shown). An increase in acetylation of both substrates of SIRT1, histone-3 and p53 (a nonhistone substrate), was found according to the decline in SIRT1 deacetylase activity. In addition, expression of p21, a downstream molecule of p53, was significantly induced by Pi as well. Quantitative assessment showed that an increase in these expression levels of acetylated (Ac)-p53 and p21 on day 3 and day 6 was statistically significant compared with the pretreatment levels, suggesting that downregulation of SIRT1 activity may mediate the subsequent increase in Ac-p53 and p21 expression.

To address whether SIRT1 downregulation-related SMC senescence and calcification are reversible or not, the effects of continuation or termination of high-dose Pi were examined. As shown in Figure 3B, the continuation of Pi up to day 10 was associated with SIRT1 downregulation and subsequent upregulation of Ac-p53 and p21, leading to induction of senescence-related calcification. However, the slight increase in senescent cells was not statistically significant, although calcification was significantly induced. Of note, the Pi-induced downregulation of SIRT1 was almost completely reversed by withdrawal (termination) of Pi stimulation (exchange of Pi from 2.6 mmol/L to 1.4 mmol/L as a normal level on day 6) as shown in Figure 3B. According to the restoration of SIRT1, levels of both Ac-p53 and p21 were also decreased without more progression. In addition, termination of Pi showed no progression of senescence-related calcification; however, preexisting senescent cells and calcification on day 6 continued without regression.

Next, NPC inhibition by PFA completely blunted Pi-induced SIRT1 downregulation and subsequent activation of its downstream p53/p21 pathway (Figure 3C).

Regulation of SIRT1 Modulates Pi-Induced SMC Senescence and Calcification

The effects of modulation of SIRT1 activity on Pi-induced cellular senescence were investigated. First, sirtinol, a chem-

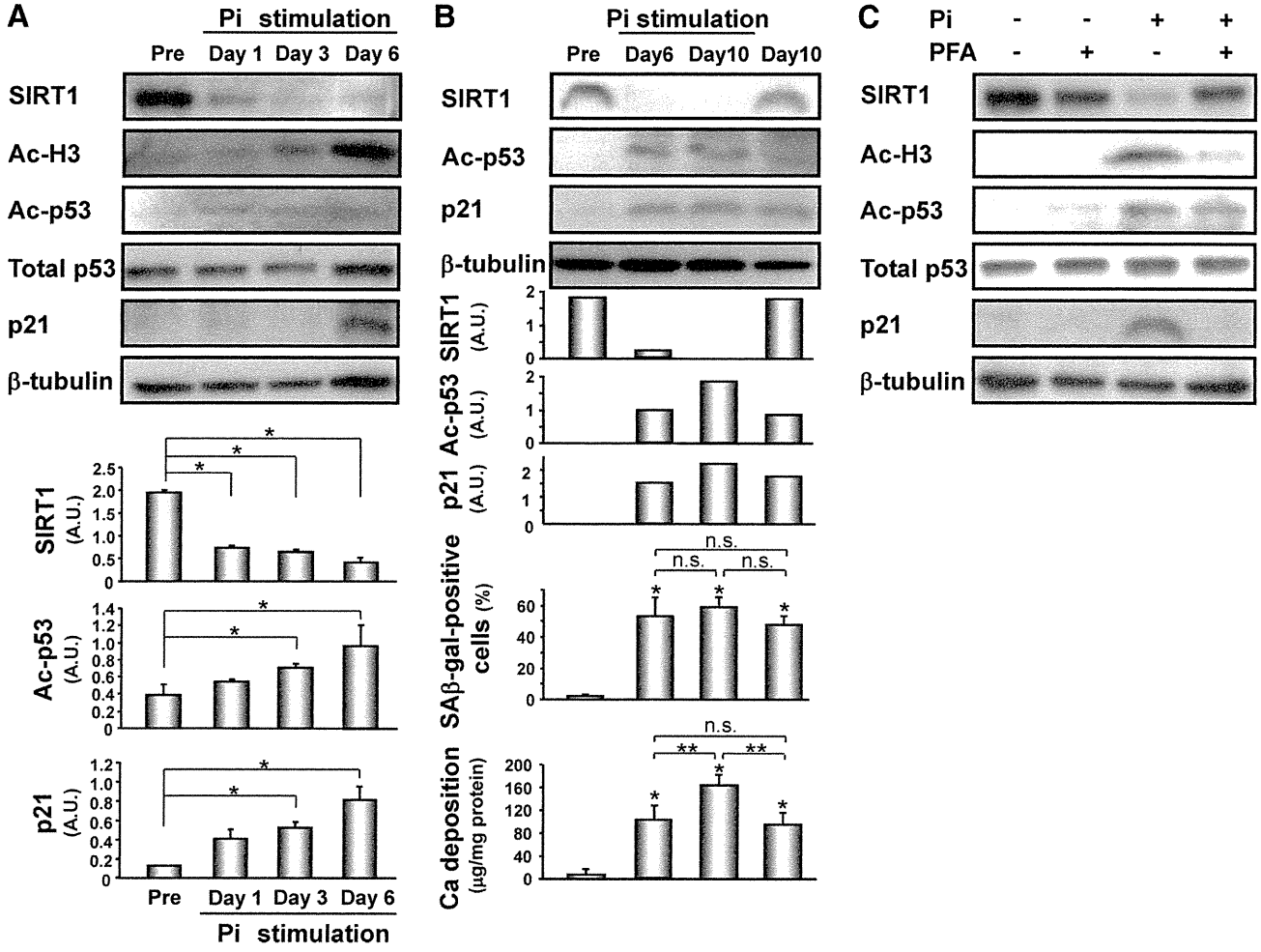

Figure 3. Inorganic phosphate (Pi) stimulation leads to sirtuin 1 (SIRT1) downregulation and subsequent p21 activation. A, The effect of Pi on SIRT1 expression and its downstream pathway was examined. Treatment of human aortic SMCs (HASMCs) with Pi (2.6 mmol/L) showed downregulation of SIRT1 expression, leading to an increase in acetylation of its substrates (acetylated [Ac]-H3 and Ac-p53) and p21 expression. Bottom: Quantitative analysis showed that Pi gradually induced not only SIRT1 downregulation but also upregulation of Ac-p53 and p21. B, To address whether SIRT1 downregulation-related senescence and subsequent calcification are reversible, the effects of continuation or termination of high-dose Pi were examined. As shown in 4th lane from left, termination (on day 6) of Pi showed no progression of senescence-related calcification in association with restoration of SIRT1, whereas continuation (up to day 10, 3rd lane from left) of Pi stimulation showed further progression of calcification. C, Treatment with phosphonoformic acid (PFA), a Na-dependent phosphate cotransporter inhibitor, completely reversed Pi-induced SIRT1 downregulation. A decline in Ac-H3 and Ac-p53 reflected the restoration of SIRT1 deacetylase activity. Pi-induced p21 activation was significantly inhibited by inhibition of Pi transport.

ical inhibitor of SIRT1, induced an increase in SAβ-gal-positive cells even under a normal Pi (1.4 mmol/L), and the increased number of senescent cells induced by Pi was significantly augmented by sirtinol (Figure 4A). Sirtinol dose-dependently augmented Pi-induced calcification, although no augmentation was found under a normal Pi (Figure 4B and 4C). Conversely, treatment with resveratrol, an activator of SIRT1, significantly reduced both Pi-induced senescent transition and calcification in a dose-dependent manner (Figure 4D to 4F).

Second, complete knockdown of SIRT1 by siRNA caused a significant increase in acetylation of both substrates (histone-3 and p53) and p21 expression (Figure 5A). Similarly to sirtinol, SIRT1 inhibition by siRNA also augmented not only senescent transition (Figure 5A, bottom) but also calcium deposition (Figure 5C, top).

Although stimulation with Ang II alone could increase the number of SAβ-gal-positive cells, it did not increase calcium deposition. To understand the mechanism of these discrepant phenomena, the effect of Ang II alone on osteoblastic phenotypic change was examined. Ang II alone did not increase the expression of Runx2 in the absence of Pi stimulation, unlike Pi stimulation (Figure 5B).

To understand the detailed mechanism by which SIRT1 modulates senescence-related calcification, the effect of SIRT1 on phenotypic change in HASMCs was examined. Pi inhibited the expression of caldesmon, a differentiated SMC lineage marker, and complete knockdown of SIRT1 augmented the Pi-induced partial downregulation of caldesmon (Figure 5C, middle). In contrast, real-time polymerase chain reaction analysis showed that Pi induced the expression of two representative osteoblastic markers, Runx-2/Cbfa-1 and alkaline phosphatase (Figure 5C, bottom) with statistical significance. In addition, complete knockdown of SIRT1 using siRNA significantly accelerated the Pi-induced os-

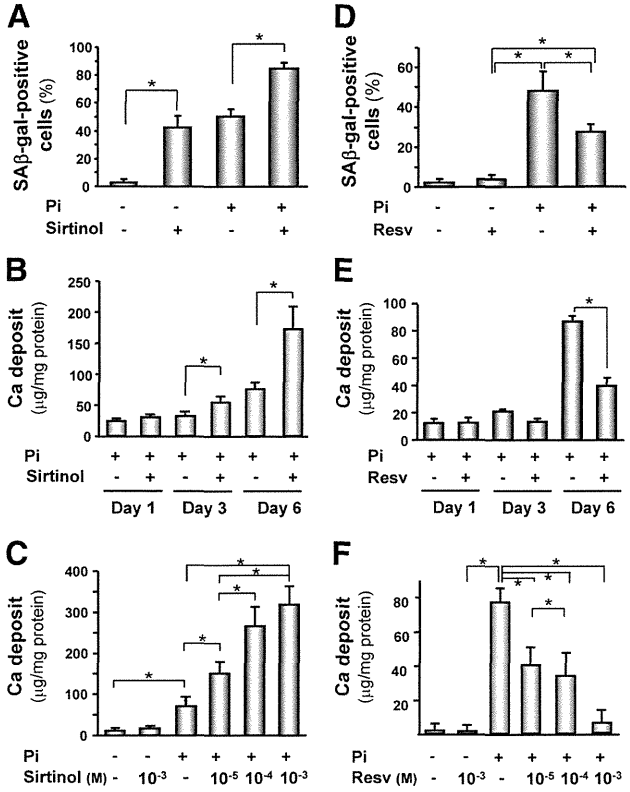

Figure 4. Modulation of sirtuin 1 (SIRT1) affects inorganic phosphate (Pi)–induced senescent phenotypic change and calcification in smooth muscle cells (SMCs). The effects of sirtinol (a chemical inhibitor of SIRT1 activity; A to C) and resveratrol (an activator of SIRT1; D to F) on Pi-induced senescent phenotypic change and calcification were examined (n=6). A, SIRT1 inhibition by sirtinol (10 μmol/L) showed an increase in the number of senescence-associated β-galactosidase (SAβ-gal)-positive cells even without Pi stimulation. The increase in Pi-induced senescence was significantly augmented by sirtinol. Sirtinol augmented Pi-induced calcium deposition in human aortic SMCs (HASMCs) in a time-dependent (B) and dose-dependent manner on day 6 (C). Conversely, treatment with resveratrol (Resv; 10 μmol/L) showed a reduction of the Pi-induced senescent phenotype (D) and calcification (E). The inhibitory effect of resveratrol on calcification was dose dependent (F).

teoblastic phenotypic change, suggesting that modulation of SIRT1 is associated with osteoblastic phenotypic change in SMCs.

Inhibition of Senescence-Related Calcification in SMCs by p21 Knockdown

To address the association of p21 with senescence-related calcification, knockdown of p21 using siRNA was performed. Treatment of p21 siRNA (up to 200 pmol/L) completely inhibited p21 (Figure 5D). p21 knockdown completely inhibited Pi-induced senescence and subsequent calcification (Figure 5E).

Regulation of NPC-Mediated Runx2 Expression by SIRT1/p21 Pathway

As the next step, the role of SIRT1 in NPC-mediated Runx2/Cbfa1 expression was examined. First, complete knockdown of SIRT1 did not show any change in both osteoblastic markers, Runx2 and alkaline phosphatase, in a normal Pi (Supplemental Figure I). As shown in Figure 5F, Pi-induced Runx2 was significantly blunted by PFA, an NPC inhibitor. SIRT1 activation by resveratrol inhibited Pi-induced Runx2 activation. The Runx2 induction was augmented by knockdown of SIRT1 by siRNA, and the activation was completely inhibited by PFA. Surprisingly, Runx2 activation was strongly inhibited by knockdown of p21 alone. In addition, the inhibition of Runx2 induction by double knockdown of SIRT1 and p21 was less than that by single knockdown of SIRT1.

To address a difference in senescent induction by Pi or Ang II, immunohistological assessment of SIRT1 in HASMCs was examined (Supplemental Figure II). Although SIRT1 was predominantly localized in nucleus without Pi, the translocation of SIRT1 to cytoplasm was observed after Pi stimulation for 24 hours, and its expression disappeared in both areas on day 6. In contrast, Ang II stimulation did not show the dynamic translocation.

High Sensitivity of SMCs With Replicative Senescence to Pi-Induced Calcification

Not only Pi-induced "premature senescence" in HASMCs but also the effects of Pi on "replicative senescence" were evaluated. Senescent cells (passage 18) were more sensitive to Pi-induced calcification compared with young cells (passage 7) (Figure 6A). SIRT1 expression was downregulated in senescent cells compared with young cells, and the downregulation was significantly augmented by Pi stimulation (Figure 6B, top). In parallel with this finding, senescent cells showed an increase in Ac-p53 and p21 expression. Statistical analyses using densitometric measurement showed that (1) downregulation of SIRT1 and upregulation of Ac-53 and p21 were augmented by replicative senescence, and (2) Pi inhibited the SIRT1-p21 pathway even in cells with replicative senescence (passage 18) (Figure 6B, bottom).

Discussion

Vascular aging, leading to cardiovascular disease, manifests complex and diverse vascular changes (eg, impairment of distensibility due to loss of arterial elasticity).[1,16] Arterial wall stiffness resulting from ectopic calcification is a complication of advanced atherosclerosis and makes the management of hemodynamics more difficult in the elderly. Few reports have addressed whether cellular senescence is associated with SMC calcification. This study showed the importance of SIRT1, a longevity gene, in arterial calcification in association with cellular senescence.

First, our data obtained from animal experiments clearly showed the association of senescent SMCs with aortic medial calcification in the renal failure rats with hyperphosphatemia. Senescent cells showed significant colocalization with calcium deposition. Intriguingly, numerous senescent cells could be detected before microscopic calcification occurred at 4 weeks after the start of renal failure induction (data not shown), suggesting that the transition to a senescent phenotype in medial SMCs may be associated with the initiation and progression of calcification. Therefore, hyperphosphatemia, a potent uremic factor, may be a stimulator to induce senescent phenotypic transition of medial SMCs.